Environment International 133 (2019) 105231

Contents lists available at ScienceDirect

Environment International

journal homepage: www.elsevier.com/locate/envint

Integration of metabolomics and transcriptomics reveals short-chain chlorinated paraffin-induced hepatotoxicity in male Sprague-Dawley rat

Ningbo Geng[a,1], Xiaoqian Ren[a,b,1], Yufeng Gong[a], Haijun Zhang[a,*], Feidi Wang[c], Liguo Xing[d], Rong Cao[a], Jiazhi Xu[a], Yuan Gao[a], John P. Giesy[e], Jiping Chen[a,*]

[a] CAS Key Laboratory of Separation Science for Analytical Chemistry, Dalian Institute of Chemical Physics, Chinese Academy of Sciences, Dalian, Liaoning 116023, China
[b] University of Chinese Academy of Sciences, Beijing 100049, China
[c] Institute of Quality and Standard for Agro-Products, Zhejiang Academy of Agricultural Sciences, Hangzhou 310021, China
[d] Safety Evaluation Center of Shenyang Research Institute of Chemical Industry Ltd, Shenyang 110021, China
[e] Toxicology Program and Department of Veterinary Biomedical Sciences, University of Saskatchewan, Saskatoon, SK, Canada

ARTICLE INFO

Handling editor: Yong-Guan Zhu

Dedicated to the 70th anniversary of Dalian Institute of Chemical Physics, CAS.

Keywords:
SCCPs
Transcriptomic
Metabolomic
PPARα
Energy metabolism

ABSTRACT

Background: Short-chain chlorinated paraffins (SCCPs) used in various industrial applications have been listed as new POPs. Previous studies based on high-dose exposures indicate their hepatotoxicity. However, their mechanisms of toxicity or adverse outcome pathways and health risks remain largely unknown.
Objectives: This study aimed to evaluate metabolic consequences of chronic dietary exposure to SCCPs at low doses and reveal the molecular mechanisms underlying hepatotoxicity of SCCPs.
Methods: A combination of transcriptomics and metabolomics, together with general pathophysiological tests were performed to assess the hepatic response of male rats exposed to SCCPs.
Results: Our results highlight two major modes of action: Inhibition of energy metabolism and activation of the peroxisome proliferator-activated receptor α (PPARα). Exposure to SCCPs suppressed oxidative phosphorylation, glycolysis, gluconeogenesis and turnover of ATP-ADP-AMP and thus results in deficiencies of amino acids and nucleotides in liver of the rat. Exposure to SCCPs affected expression levels of 13 genes downstream of PPARα that encode proteins associated with metabolism of fatty acids. As a result, peroxisomal and mitochondrial fatty acid *β*-oxidation, microsomal fatty acid *ω*-oxidation, and lipogenesis were accelerated.
Conclusions: Results of this work strongly support the conclusion that low-dose exposure to SCCPs can result in adverse outcomes in the rat model. Significant SCCP-induced inhibition of energy metabolism occurs at environmentally relevant dosages, which suggests that SCCPs exhibit metabolic toxicity. Interactions of SCCPs with PPARα signaling pathway can explain the disruption of lipids and amino acids metabolism.

1. Introduction

Short-chain chlorinated paraffins (SCCPs) are mixtures of polychlorinated *n*-alkanes with 10–13 carbon atoms. As a constituent of chlorinated paraffins, SCCPs are widely used in various industrial applications, including plasticizers, flame retardants, metal-working fluids, lubricant additives, paints and sealants (Fiedler, 2010). Due to their environmental persistence, bioaccumulation potential, long-range transport potential and adverse health effects, in 2017, SCCPs were listed in Annex A of the Stockholm Convention on Persistent Organic Pollutants (POPs) (Ali and Legler, 2010; Hüttig and Oehme, 2005; Li et al., 2016; Wei et al., 2016). Annual production of SCCPs worldwide in 2016 was estimated to exceed 165,000 tons (Gluge et al., 2016). As a result of the production and the wide variety of industrial applications, SCCPs have been ubiquitously detected in environmental matrixes and human body (Wei et al., 2016; Thomas et al., 2006; Xia et al., 2017; Li et al., 2017), posing potential hazards to wildlife and humans.

SCCPs exhibit little potency for acute toxicity in animals but are potentially carcinogenic (Bucher et al., 1987). In sub-chronic studies of toxicity to rats and mice, SCCPs produced toxic effects on liver, kidney, thyroid, and parathyroid glands (Nielsen and Ladefoged, 2013). The no- and lowest-observed adverse effect levels (NOAEL and LOAEL) of SCCPs were 10 and 100 mg/kg body mass (bm)/d for rats, respectively (UNEP, 2011). Exposure to SCCPs results in up-regulated expression of some cytochrome P450 family genes (Zhang et al., 2016), which alters intracellular redox status (Geng et al., 2015). SCCPs have been reported

* Corresponding authors at: Dalian Institute of Chemical Physics, Chinese Academy of Sciences, 457 Zhongshan Road, Dalian 116023, China.
E-mail addresses: hjzhang@dicp.ac.cn (H. Zhang), chenjp@dicp.ac.cn (J. Chen).
[1] These authors contributed equally to this work.

https://doi.org/10.1016/j.envint.2019.105231
Received 26 July 2019; Received in revised form 24 September 2019; Accepted 27 September 2019
Available online 01 November 2019

to induce peroxisome proliferation, which is associated with damage to liver (Wyatt et al., 1993). Moreover, SCCPs function as endocrine disruptors. Based on results observed during *in vivo* studies, exposure to SCCPs reduces concentrations of free thyroid hormone and disrupts thyroid signaling, although the thyroid gland is not a direct target of SCCPs (Liu et al., 2016; Gong et al., 2018). Additionally, a recent *in vitro* study has also shown that SCCPs not only exert their endocrine-disrupting effects through estrogen receptor α and the glucocorticoid receptor, but also alter 17 β-estradiol and release of cortisol (Zhang et al., 2016). These endocrine-disrupting effects, together with oxidative stress, imply that SCCPs might cause adverse effects to health, even at low doses. Currently data are insufficient to comprehensively assess the biological events caused by SCCPs, and very limited information is available regarding their toxic effects at environmentally relevant dosages or internal concentrations in tissues of humans.

The correlation between exposure to endocrine disruptors and their effects on health is often difficult to determine, mainly due to the occurrence of low-dose effects and non-monotonic dose-responses (Vandenberg et al., 2012). However, the advent of omics technologies has made these analyses possible. Transcriptomics identifies broad-scale changes in expression levels of genes, which might help researchers ascertain specific, molecular responses as endpoints of low-dose effects and lead to the generation of hypotheses about the mechanisms of action (Shi et al., 2006). Metabolomics can reveal system-wide alterations in metabolic pathways in response to low-dose exposure and facilitate identification of early biomarkers of a toxicant (Spivey, 2004). It was hypothesized that SCCPs initiate specific biological events and disturb global metabolism at exposures relevant to concentrations observed in tissues of humans or environmental matrices. The present study was designed to test this hypothesis in the liver of male Sprague-Dawley (SD) rats using a combination of transcriptomic and metabolomic approaches.

In this study, exposure to 0.01 mg SCCP/kg body mass/day (kg bm/d) was selected as low dose, which is comparable to the human daily exposure level of SCCPs, specifically via infant lactational exposure: 0.34–8.65 μg/kg bm/d (Cao et al., 2017; Xia et al., 2017), inhalation exposure: < 0.01–5.9 μg/kg bm/d (Friden et al., 2011; Shi et al., 2017), dietary exposure: 0.32–1.1 μg/kg bm/d (Cao et al., 2015; Gao et al., 2017), occupational exposure: 40.7, 22.6, and 62.2 μg/kg bm/d for workers, local adults and children in a mega e-waste recycling industrial park with high end exposure (Chen et al., 2018). The dose of 1 mg/kg bm/d was selected as middle dose. The LOAEL of 100 mg/kg bm/d was adopted as a positive control dose (high dose) to link the low-dose effects with the known deleterious outcomes of SCCP exposure. The hepatic responses of male SD rats exposure to SCCPs were characterized by use of transcriptomics and metabolomics, together with general pathophysiological endpoints. The goal was to identify multiple targets affected by SCCPs and to determine some early responses.

2. Methods

2.1. Chemicals

SCCPs used in the present study were a mixture of $C_{10–13}$-CPs (chlorine content: 56.5% by mass; purity: > 99.9%) synthesized by chlorination of $C_{10–13}$-*n*-alkanes (C_{10}:C_{11}:C_{12}:C_{13} = 1:1:1:1, mass ratio) in our laboratory. The chromatographic profile of prepared SCCPs was similar to that of a SCCP standard (55.5% Cl) obtained from Dr. Ehrenstorfer (Augsburg, Germany) (Fig. S1). HPLC-grade acetonitrile (ACN) and methanol were obtained from Fisher (Fair Lawn, NJ, USA). Ammonium acetate and formic acid were obtained from J&K Scientific (Beijing, China). The water used in all experiments was ultrapure water from a Milli-Q system (Millipore, Billerica, MA, USA). Six internal standards (1,2-diheptadecanoyl-*sn*-glycero-3-phosphoethanolamine, octanoyl (8,8,8-D3)-L-carnitine, 1-lauroyl-2-hydroxy-*sn*-glycero-3-phosphocholine, hendecanoic acid, L-phenylalanine-d5 and nonadecanoic acid) were purchased from Sigma-Aldrich (Sigma Chemical Co, USA). Internal standards were dissolved into methanol before metabolites extraction.

2.2. Animal experiment

All animal experiments were performed according to protocols approved by the Institutional Animal Care and Use Committee in the Safety Evaluation Center, Shenyang Research Institute of Chemical Industry, China. Male SD rats (8 weeks old; with weight ranging from 339 to 407 g) were housed in a controlled environment at a temperature of 25 ± 3 °C on a 12-h light/dark cycle. After 5 d of acclimation, rats were randomly assigned to one of four groups, each containing ten animals. SCCPs were administered to rats at various doses (0, 0.01, 1 and 100 mg/kg bm/d) for 28 d. In the exposure groups, SCCPs were dissolved in corn oil and administered by gavage, while the control group received corn oil only. Body mass was monitored and recorded every 4 d throughout the experiment. Rats were euthanized humanely under diethyl ether anesthesia after 28 days of exposure. Blood and urine were collected for clinical chemistry and hematology analyses. Livers were surgically removed and weighed. A fraction of the livers was fixed with a 10% formalin solution containing neutral phosphate-buffered saline for the histopathological examination; the remaining tissues were frozen in liquid nitrogen and stored at –80 °C for the quantification of gene expression and metabolite levels.

2.3. Pathophysiological test

Sixty-one hematological and biochemical parameters were measured using an automated hematology analyzer (Sysmex XT-2000i, Japan), a biochemical blood analyzer (Hitachi 7180, Hitachi, Japan) and an automated urine analyzer (Uritest-500B, China). The investigated hematological and biochemical parameters are shown in Tables S1–3. Liver tissues were embedded in paraffin, stained with hematoxylin and eosin, and examined under a light microscope (Axio Imager A1, Germany).

2.4. Exposure estimation

SCCPs were measured in liver collected after 28 days of oral administration. Samples were analyzed using previously published methods (Gao et al., 2011) that involved extraction, cleanup and final determination performed on a trace gas chromatograph coupled to a Trace DSQ II mass spectrometer in ECNI mode (GC/ECNI-MS, Thermo, USA). Approximately 100 mg of the liver samples were extracted with ultrasonic solvent extraction, purified on a multilayer silica gel column, then evaporated and redissolved in 20 μL of the internal standard solution ($^{13}C_6$-α-HCH in *n*-nonane) for the instrumental analysis. Chromatographic separation was performed with a capillary DB-5 column (J &W Scientific, USA). Three samples from each group were subjected to the quantitative analysis, and the concentrations of SCCPs were normalized to mass of liver.

2.5. Transcriptomic analysis

Livers from four rats in each treatment group were randomly selected for transcriptomic analysis. Total RNA was isolated using the mirVana™ miRNA Isolation Kit (Ambion, US) and subsequently amplified and labeled with cyanine-3 (Cy3) by use of the Low Input Quick Amp Labeling Kit, the microarray analysis was performed with whole rat genome 4 × 44 K arrays. Briefly, each slide was hybridized with 1.65 μg of Cy3-labeled cRNA for 17 h, washed in staining dishes, and scanned on an Agilent Microarray Scanner (Agilent Technologies, US).

Eight significant differentially expressed genes (DEGs) (*Cdk1*, *Ednra*, *Pfkfb1*, *Slpi*, *Herpud1*, *Acaa1b*, *Alas1* and *Acot2*) were selected for

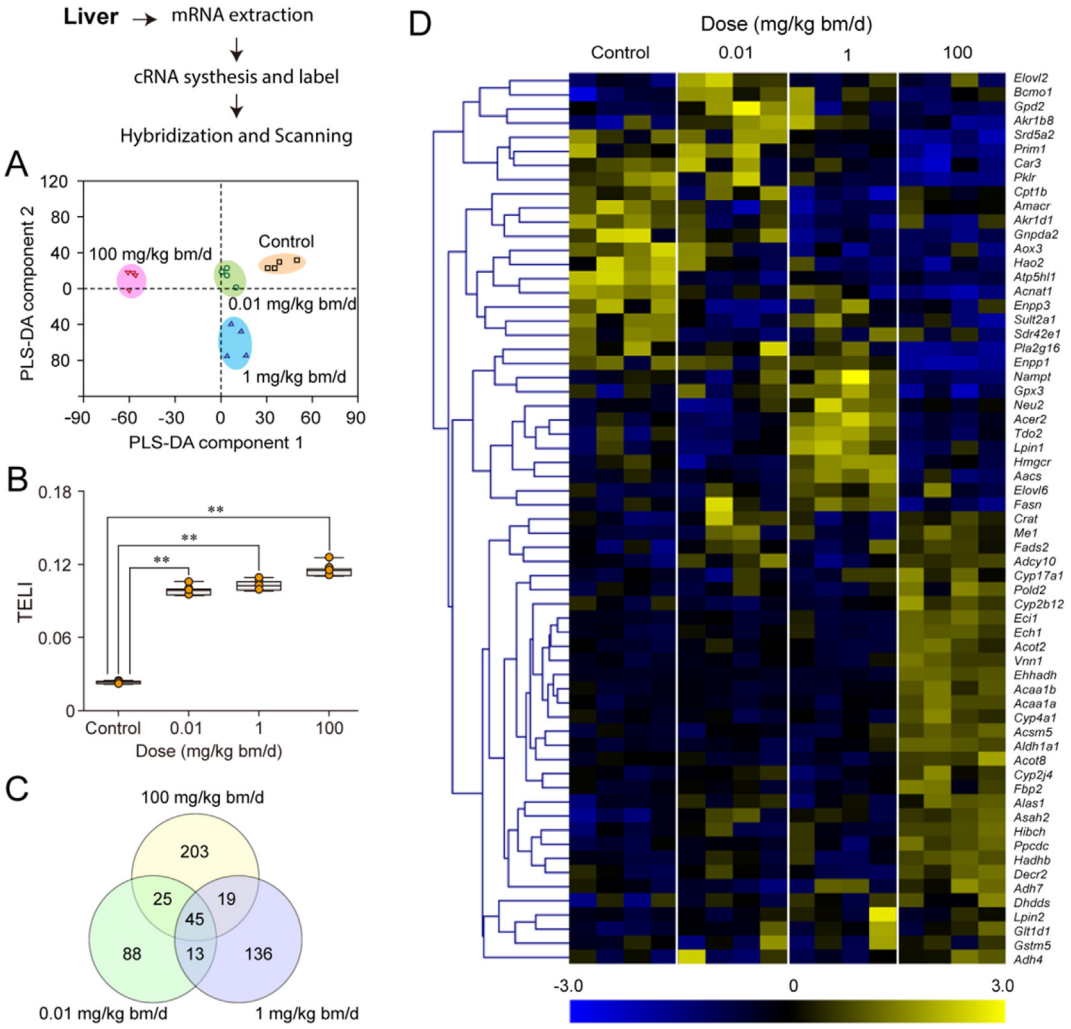

Fig. 1. Divergence in expression levels of genes and metabolism-related alteration on transcriptional level of SD rat liver after 28-day oral administration of SCCPs. (*A*) PLS-DA score plot of the genes identified from the control and SCCP-treated groups. (*B*) TELI of liver transcription fingerprint in the control and SCCP-treated groups. (*C*) The Venn diagram shows the DEGs overlap among the three SCCP-treated groups. (*D*) Hierarchical clustering based on the DEGs related to metabolism. *, $P < 0.05$; **, $P < 0.01$.

validation of quantitative real-time polymerase chain reaction (qRT-PCR) using the ABI power SYBR green PCR master mix (ABI, USA). Amplification was performed using a 7900 HT Sequence Detection System (ABI, USA), and a melting curve analysis was performed to confirm specificity of qRT-PCR. Detailed information about the transcriptomic analysis is provided in Supplemental Material, Gene expression analysis.

2.6. Metabolomic analysis

Livers from ten rats in each group were used for metabolomics analysis, samples of each liver (100 mg) were mixed with 1 mL of H_2O respectively, homogenized, and then ultrasonicated for 5 min in an ice-water bath. Samples were subsequently freeze-dried and extracted with a mixture of methanol/water (4:1, v:v). The resulting solution was vortexed for 30 min and then centrifuged at 13,000*g* for 20 min at 8 °C. Finally, the supernatant was filtered through an organic phase filter and transferred to a vial for the metabolite analysis. Prior to extraction, six internal standards were spiked into the sample for quality control of the sample preparation and instrumental analysis.

A pseudotargeted approach was adopted for the metabolomic analysis. This approach exhibited greater repeatability and wider linear range than the traditional untargeted metabolomic method. Briefly, rat liver extracts were analyzed on a Waters Acquity ultra-performance liquid chromatography coupled online to an ABI Q-Trap 5500 (AB SCIEX, USA) system (UPLC/Q-Trap MS) operated in multiple reaction monitoring (MRM) mode, for which the MRM ion pairs were acquired from the liver extracts through untargeted tandem MS using an Agilent 1290 Infinity ultra-performance liquid chromatography system coupled online to an Agilent 6540 Q-TOF MS (Agilent, Santa Clara, CA) system (UPLC/Q-TOF MS). The same liquid chromatography conditions were employed for both UPLC/Q-Trap MS and UPLC/Q-TOF MS. Six hundred eighty-eight ion pairs with defined parameters were monitored. The details of the instrumental analyses are shown in Supplemental Material, LC-MS-based metabonomics analysis.

2.7. Data processing

Statistical differences were performed by using Student's *t*-test for comparisons between two groups or One-Way ANOVA for multiple comparisons with Duncan's method. The normality assumption and variance homogeneity tests were performed before ANOVA. Hierarchical cluster analysis (HCA) was conducted using MeV software. Principal component analysis (PCA) and partial least squares discriminate analysis (PLS-DA) were applied with unit variance (UV) scaling using SIMCA-P 11.5 (Umetrics, Sweden). The VIP value of every

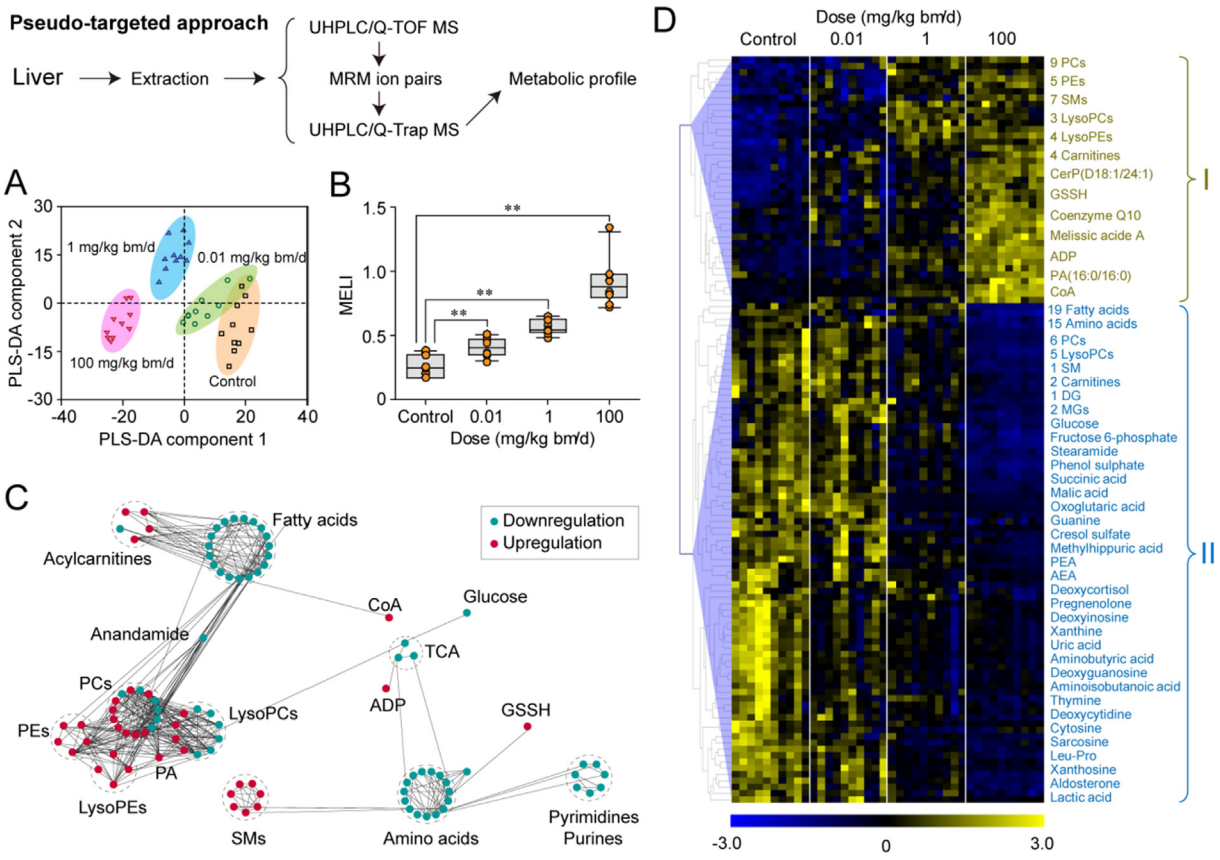

Fig. 2. Changes in metabolic profile of SD rat liver after 28-day oral administration of SCCPs. (*A*) PLS-DA score plot of liver metabolites after exposed to SCCPs at various doses. (*B*) MELI of liver metabolism fingerprint in the control and SCCP-treated groups. (*C*) Metabolic correlation networks of the differential metabolites and related pathways. SM: sphingomyelin; PC: phosphatidyl choline; LysoPC: lysophosphatidyl choline; PE: phosphatidyl ethanolamine; LysoPE: lysophosphatidyl ethanolamine; PA: phosphatidic acid; CoA: coenzyme A; GSSH: oxidized glutathione; ADP: Adenosine diphosphate. (*D*) Hierarchical clustering based on the differential metabolites with P value of < 0.05 base on one-way ANOVA and VIP value of > 1, PEA:Palmitoylethanolamide; AEA: Anandamide; Leu-pro: Leucylproline; MG: monoacyl glycerol; DG: diacyl glycerols. *, $P < 0.05$; **, $P < 0.01$.

metabolite ion is also calculated by SIMCA-P.

Microarray gene expression data were extracted with feature extraction software 10.7 (Agilent), normalized by GeneSpring software 11.0 (Agilent). Background corrected signal was used and raw data were normalized by Quantile algorithm. MultiQuant software 3.0 (AB SCIEX) was used for metabolomic data processing of the Q-Trap MS data. The correlation network of metabolites was constructed using the Cytoscape software package (version 2.8.2). The transcriptional effect level index (TELI) and metabolic effect level indexes (MELI) were calculated to describe the dose-response behavior of SCCP exposure. Detailed calculation methods are shown in the Supplemental Material, Determination of TELI and MELI. Integrated enrichment analysis and pathway-based visualization of transcriptomic and metabolomic data were conducted using IncroMap software 1.7 according to the Kyoto Encyclopedia of Genes and Genomes (KEGG) pathway database, metabolism-related pathways with enrichment P values < 0.05 were selected and further sorted according to the pathway impact.

3. Results

3.1. SCCPs-induced changes in gene expression

Profiles of transcriptomic results for livers of male rats were analyzed using cRNA microarrays. After removing unannotated and repeated entities, a total of 10,144 genes were identified for which gene symbols were available. PLS-DA was performed to estimate differences in expression of identified genes among groups, the R^2 and Q^2 were 0.993 and 0.73 respectively. In the PLS-DA score plot, the first component (PC1) distinguished the high-dose group from the other dosed groups, and the middle-dose group was clearly separated from the control group by the second component (PC2). The low-dose group and control group both had positive scores for PC1 and PC2 (Fig. 1A). Nevertheless, these groups were also distinct from each other. To verify the results of the microarray analysis, eight differentially expressed genes were selected randomly for validation and quantification by qRT-PCR. Overall, the qRT-PCR results closely paralleled patterns of expression observed in the microarray data (Table S4).

Significantly greater values of TELI were observed with increased dosages of SCCPs (Fig. 1B), which suggested that exposure to SCCPs caused perturbation of transcription, even at the low dose (0.01 mg/kg bm/d). After removing mRNA with low signal intensity, pairwise comparisons base on *t*-test were conducted to identify DEGs between the control and rats exposed to SCCP. Genes displaying differences in expression with a P value of < 0.05 and a fold change (FC) cut-off of > 1.5 were considered DEGs, after a 28-d exposure, 171, 213 and 292 genes were identified to be DEGs in livers of rats exposed to 0.01, 1 or 100 mg/kg bm/d SCCPs, respectively (Fig. 1C).

A KEGG pathway enrichment analysis was then performed to determine the association of all DEGs with metabolic processes occurring in the rat livers, 63 DEGs were identified to be genes encoding hepatic enzymes (Table S5). Among these genes, 15, 20 and 42 were observed in rats exposed to 0.01, 1 or 100 mg SCCPs/kg bm/d, respectively. A heatmap of the hierarchical clustering analysis of DEGs encoding hepatic enzymes demonstrated three major dose-response trajectories (Fig. 1D). Expression levels of all 15 DEGs, encoding for enzymes involved in fatty acid metabolism were up-regulated in response to

exposure to SCCPs, whereas expression levels of four DEGs, encoding enzymes related to purine and pyrimidine metabolism, *Enpp1*, *Enpp3*, *Prim1* and *Pklr*, were reduced in livers of rats exposed to SCCPs. Non-monotonic trends were observed for *Elovl2*, *Elovl6*, *Fasn*, *Lpin1* and *Lpin2*.

3.2. SCCP-induced changes in metabolic profiles

A PLS-DA was performed on all analyzed metabolites to estimate the metabolic variance induced by various doses of SCCPs. The R^2 and Q^2 were 0.979 and 0.69 respectively. In the PLS-DA score plot, rats exposed to the middle and high doses were clearly separated from the control group, whereas rats exposed to the low dose exhibited a slight overlap with the control group (Fig. 2A). Values of MELI exhibited a significant and dose-dependent increase with SCCPs (Fig. 2B), which suggested that SCCP exposure perturbed normal metabolic pathways even at dose of 0.01 mg/kg bm/d.

Among all doses, 328 metabolites exhibited statistically significant (one-way ANOVA) differences at P values < 0.05 and variable importance projection (VIP) value of > 1. Among these metabolites, based on pairwise comparisons with the control group, 127, 242 and 328 metabolites were significantly ($P < 0.05$) different metabolites (DMs) in livers of rats exposed to 0.01, 1 and 100 mg SCCPs/kg bm/d, respectively. The molecular structures of 118 DMs were reliably identified by MS/MS, and some were further confirmed using authentic standards (Table S6), a hierarchical clustering analysis of these identified DMs between groups indicated two major dose-response trajectories (Fig. 2D). In trajectory I, concentrations of oxidized glutathione (GSSH), coenzyme A (CoA), adenosine diphosphate (ADP) and most phospholipids were up-regulated in livers of rats exposed to all doses of SCCPs. In trajectory II, concentrations of almost all fatty acids, amino acids, purines, pyrimidines, intermediate metabolites in the tricarboxylic acid (TCA) cycle and glucose were lower in livers of rats exposed to SCCPs, relative to that in unexposed, control rats.

In a correlation network diagram constructed by pairwise computation of Pearson correlations between DMs involved in the same KEGG metabolic pathway (Fig. 2C). DMs were mainly connected by PCs, fatty acids and amino acids. Among differentially altered phospholipids, concentrations of PEs, LysoPEs and SMs were increased in response to SCCP exposure. However, PCs, LysoPCs and acylcarnitines exhibited different patterns. Concentrations of PCs linked to fatty acids were decreased, whereas concentrations of PCs linked to PEs and LysoPEs were greater in rats exposed to SCCPs.

3.3. Integrated enrichment analysis of transcript and metabolite profiles

Integrated enrichment analysis indicate that exposure to SCCPs perturbed metabolism of linoleic acid, glycerophospholipid, sphingolipids and 2 pathways of amino acid (Cys and Met metabolism, Gly, Ser and Thr metabolism), even at low dose of 0.01 mg SCCPs/kg bm/d (Fig. 3). Nucleotide metabolism and unsaturated fatty acid biosynthesis were also identified as the most relevant pathways affected by SCCPs at middle dose. carbohydrate metabolism, fatty acid degradation and peroxisome function were also significantly perturbed by SCCPs at high dose. Metabolic disorders in livers of rats fed 0.01 or 1 mg/kg bm SCCPs/d were mainly characterized by changes in metabolome, whereas in livers of rats fed 100 mg SCCPs/kg bm/d, the metabolic disorder was caused by changes in transcriptome and metabolome.

3.4. Lipid metabolism alterations

Metabolomic and transcriptomic analyses demonstrated effects of SCCPs on lipid metabolism. Interconnected pathways included glycerophospholipid metabolism, α-linoleic acid metabolism, sphingolipids and arachidonic acid metabolism as well as elongation, biosynthesis and degradation of fatty acids (Fig. 4A). Concentrations of total fatty

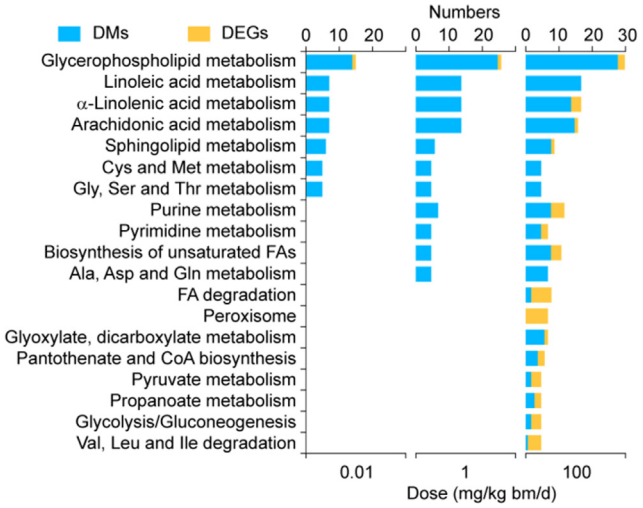

Fig. 3. Most relevant metabolic pathways perturbed by exposure to SCCPs at various doses based on the integrated enrichment analysis of transcript and metabolites.

acids (Σfatty acids) were inversely proportional to dose of SCCPs (Fig. 4B), whereas concentrations of total phospholipids (Σphospholipids) were directly proportional to dose of SCCPs (Fig. 4C). No significant difference was observed for total concentrations of acylcarnitines (Σacylcarnitines; Fig. 4D). Specifically, the ratio of ω-6 fatty acids to ω-3 fatty acids (ω-6/ω-3 ratio) was significantly greater in rats exposed to all doses of SCCPs, in a dose-dependent manner (Fig. 4E).

Degradation of fatty acids was greater in livers of rats exposed to SCCPs as Σfatty acids in livers of rats fed 1 and 100 mg SCCPs/kg bm/d were significantly less by 29.5% and 42.3%, respectively. In livers of rats dosed with 100 mg SCCPs/kg bm/d, expression levels of several genes encoding enzymes involved in fatty acid *β*-oxidation and *ω*-oxidation were significantly greater than those of controls. Exposure to SCCPs also up-regulated the expression levels of the *Elovl2* and *Elovl6* genes, which encode fatty acid elongases, *Acot2*, which encodes acyl-CoA thioesterase 2, and *Fasn*, which encodes a fatty acid synthase. Expression levels of two genes involved in arachidonic acid metabolism, *Cyp2b12* and *Cyp2j4*, were up-regulated. Transformation of α-linoleic acid to stearidonic acid might be accelerated by up-regulation of *Fads2*.

SCCPs also disrupted metabolism of glycerophospholipid and sphingolipid. In glycerophospholipid metabolism, significantly higher concentrations of phosphatidate were observed in livers of rats fed 1 or 100 mg SCCPs/kg bm/d than in controls. Expression levels of *Lpin1* and *Lpin2*, which encode phosphatidate phosphatases, were significantly increased in livers of rats dosed with 1 or 100 mg SCCPs/kg bm/d. Moreover, transformations of PCs and PEs to LysoPCs and LysoPEs were significantly altered (Fig. 4A and Fig. S3), which might be due to down-regulated expression of *Pla2g16*, which encodes phospholipase A2. In sphingolipid metabolism, concentrations of SMs were greater in all rats exposed to SCCPs and expression levels of *Acer2* and *Asah2*, which encode alkaline ceramidase 2 and neutral ceramidase, respectively, were significantly up-regulated in livers of rats fed 1 or 100 mg/kg bm/d, respectively. In addition, expression of *Neu2*, which encodes neuraminidase 2, was also up-regulated in livers of rats exposed to 1 mg SCCPs/kg bm/d.

3.5. Amino acid metabolism alterations

Results of metabolomic analyses indicated depletion of amino acids in livers of rats exposed to SCCPs. Concentrations of total amino acids (Σamino acids) in livers of rats exposed to SCCPs, were significantly decreased by more than 20% (Fig. 5A). The most relevant pathways for amino acid metabolism altered by exposure to SCCPs were alanine,

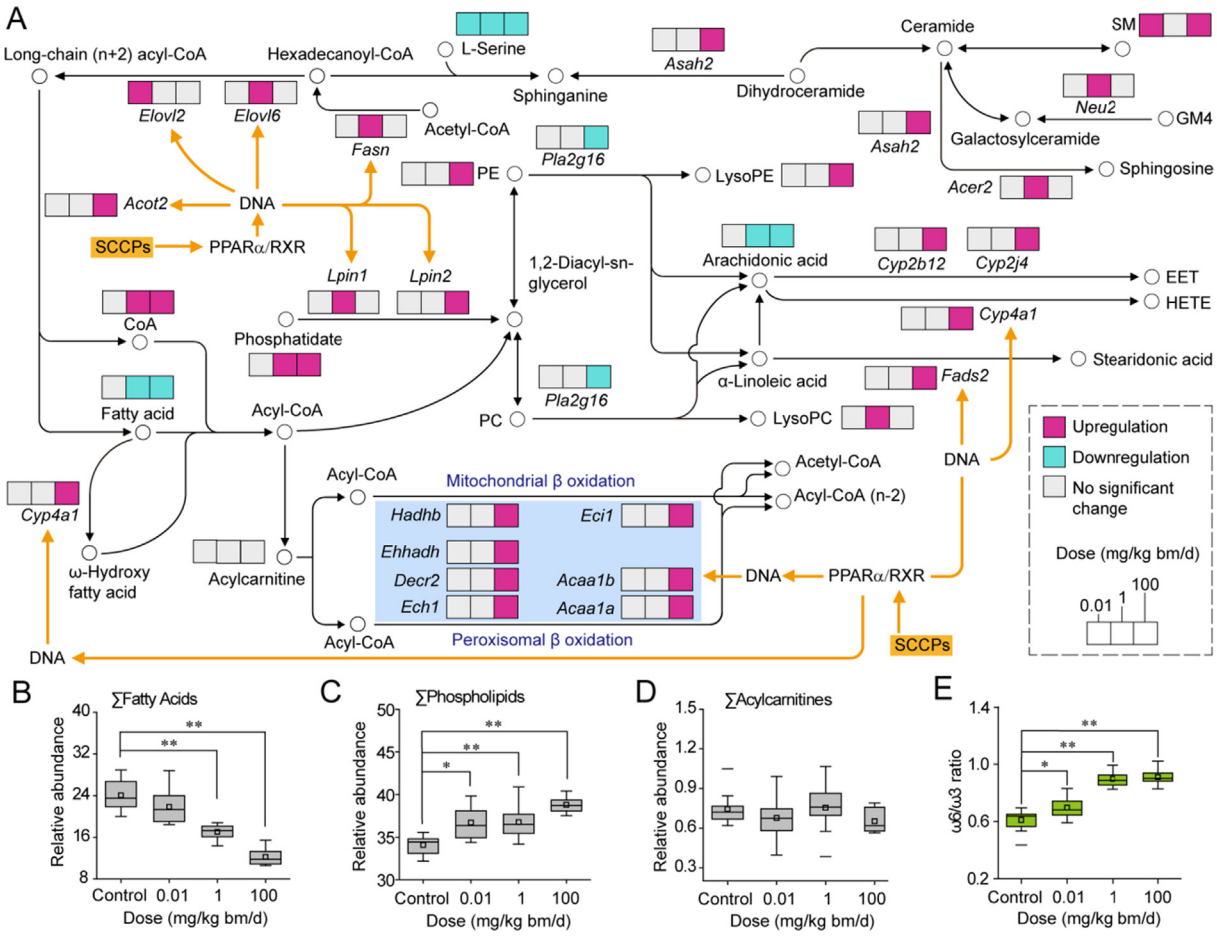

Fig. 4. Disorder of lipid metabolism in liver of SD rat after 28-day oral administration of SCCPs. (*A*) Lipid metabolism featuring the most relevant metabolites and genes perturbed by SCCPs. Statistically significant changes in metabolites and gene expression are shown in the boxes as red (up-regulation) or green (down-regulation). Genes were shown in italic to distinguish with metabolites. (*B*), (*C*) and (*D*) variation tendency of total fatty acids, total phospholipids and total acylcarnitines in liver tissue from control and SCCPs exposure rats. (*E*) Polyunsaturated fatty acids *ω*-6/*ω*-3 ratio in liver tissue of rats increased for three SCCPs exposure groups. *, $P < 0.05$; **, $P < 0.01$.

aspartate and glutamate metabolism; glycine, serine and threonine metabolism (Fig. 5B). However, results of transcriptomic analyses identified only one DEG that directly regulates amino acid metabolism, expression of *Alas1*, which encodes 5′-aminolevulinate synthase 1, was significantly up-regulated in livers of rats exposed to 0.01 and 100 mg/kg bm/d groups.

During catalysis by glutathione (GSH) synthase, glycine is transformed to GSH by linking it to L-γ-glutamylcysteine. Although concentrations of glycine and GSH in rat livers were not significantly altered by SCCP exposure, concentrations of GSSH were significantly increased in all three SCCP-treated groups. Moreover, expression of *Gpx3*, which encodes glutathione peroxidase 3 that catalyzes the transformation of GSH to GSSH, was significantly increased in rats exposed to 1 mg SCCPs/kg bm/d (Fig. 5B). In addition, by increasing the glutathione S-transferase capacity for the purpose of detoxification, exposure to SCCPs accelerated conjugation of GSH to SCCP to form SCCP-S-glutathione (Buryskova et al., 2006). Expression of Gstm5, which encodes the enzyme glutathione S-transferase mu 5 that catalyzes conjugation of GSH to organic halides (RXs) to form R-S-glutathione, was significantly increased in livers of rats exposed to 100 mg SCCPs/kg bm/d, relative to that in livers of rats in the control group.

3.6. Carbohydrate metabolism alterations

Exposure to SCCPs resulted in decreased glycolysis/gluconeogenesis. Concentrations of glucose were significantly decreased in livers of rats exposed to 100 mg SCCPs/kg bm/d, and concentrations of L-lactate were decreased in livers of rats exposed to 1 or 100 mg SCCPs/kg bm/d. In addition, expressions of *Fbp2* and *Pklr*, which encodes fructose-bisphosphatase 2 and pyruvate kinase, were significantly decreased in livers of rats exposed to 100 mg SCCPs/kg bm/d.

Regarding the TCA cycle, concentrations of succinate and 2-oxoglutarate exhibited a decreasing trend in rats exposed to SCCPs, and concentrations of malate were less in livers of rats exposed to 1 or 100 mg SCCPs/kg bm/d groups, which suggested that SCCPs suppressed the central hub of oxidative metabolism. However, pyruvate metabolism and propanoate metabolism might be enhanced by exposure to SCCPs, mainly via up-regulation expression of the *Me1* gene, which encodes malate dehydrogenase, the *Ehhadh* gene, which encodes enoyl-CoA hydratase, and the *Hibch* gene, which encodes 3-hydroxyisobutyryl-CoA hydrolase. Among these three genes, *Me1* and *Ehhadh* are both target genes of PPARα (Burri et al., 2010; Ehara et al., 2015). In addition, the levels of CoA were significantly increased in livers of rats exposed to middle and high dose of SCCPs, which should accelerate the synthesis and oxidation of fatty acids. All of these effects would result in overall suppression of the TCA cycle. The elevated concentrations of CoA might result from induction of the expression of the *Ppcdc* gene, which encodes phosphopantothenoylcysteine decarboxylase (Fig. 5B).

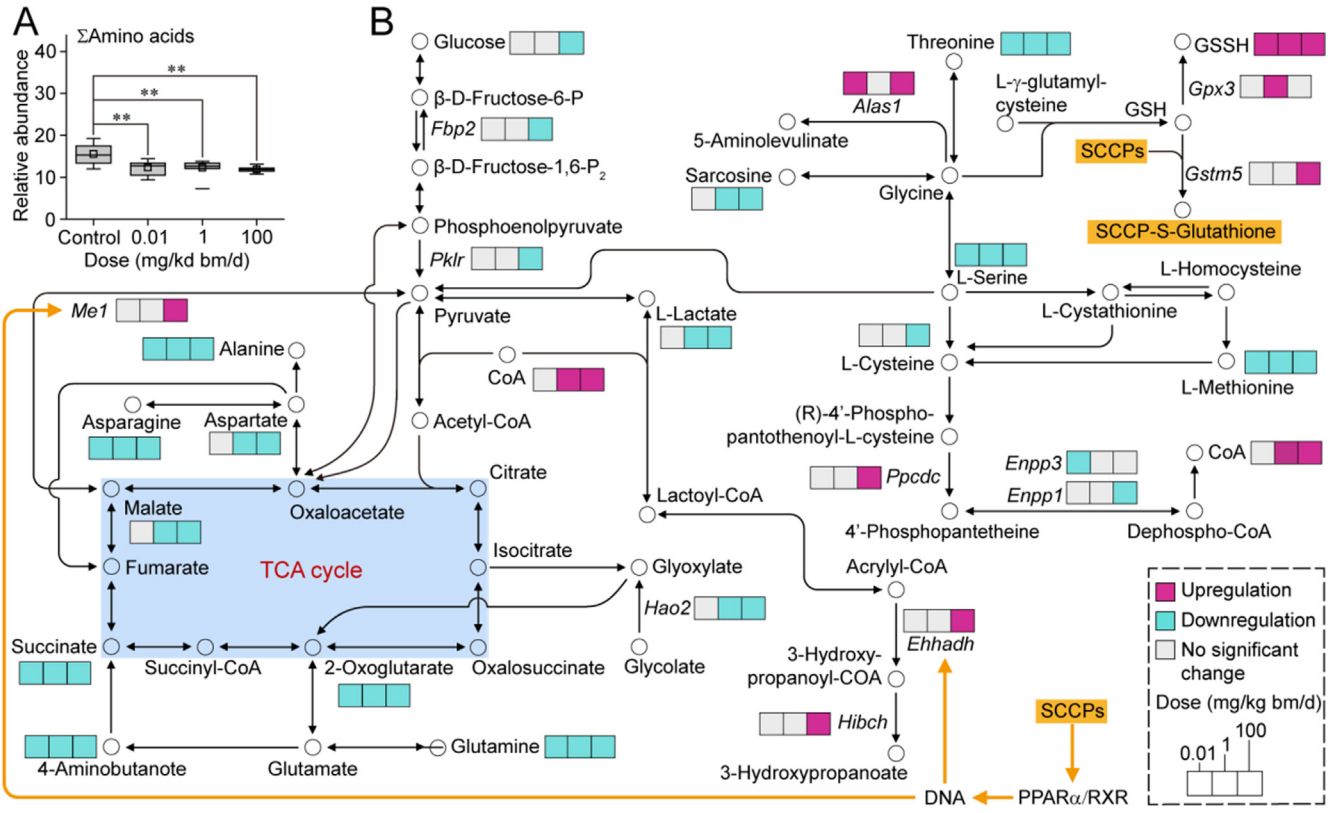

Fig. 5. Disorder of amino acid and carbohydrate metabolism in liver of SD rat after 28-day oral administration of SCCPs. (*A*) Total concentrations of amino acids (ΣAmino acids) in liver of SD rat of the control group and three doses of SCCPs. (*B*) Most relevant amino acids perturbed by SCCPs on the basis of the pathway enrichment analysis. GSH: glutathione, GSSH: oxidized glutathione, **, $P < 0.01$.

3.7. Nucleotide metabolism alterations

Total concentrations of pyrimidines (Σpyrimidines) were significantly decreased in livers of rats exposed to SCCPs, and total concentrations of purines (Σpurines) were significantly decreased in 1 or 100 mg SCCPs/kg bm/d (Fig. 6A and B), which suggests that exposure to SCCPs disrupts nucleotide metabolism. In pyrimidine metabolism, concentrations of cytosine and thymine were both significantly reduced by more than 30% in livers of rats exposed to SCCP, compared to the controls. In purine metabolism, concentrations of guanine, xanthosine, xanthine, uric acid, and deoxyinosine were all 50% less in livers of rats exposed to 100 mg SCCPs/kg bm/d. However, results of the transcriptomic analysis did not identify any DEGs that directly regulate transformation of pyrimidines or purines (Fig. 6C). Only two DEGs that regulate replication and repair of DNA were observed in livers of rats exposed to 100 mg SCCPs/kg bm/d. Expression of *Prim1*, which encodes DNA primase subunit 1, was significantly decreased, whereas expression of *Pold2*, which encodes DNA polymerase delta subunit 2, was significantly greater in rats exposed to SCCPs.

Exposure to SCCPs inhibited ATP turnover (Fig. 6C). Decreased expression of *Enpp1* and *Enpp3* genes, both of which encode ectonucleotide pyrophosphatases, suggests that transformation of ATP to adenosine monophosphate (AMP) or ADP was inhibited by SCCPs. Increased concentrations of ADP and down-regulated expression of the *Atp5hl1* gene, encoding ATP synthase, indicated that conversion of ADP to ATP was also inhibited by SCCPs. Moreover, the expression of the *Pklr* encoding pyruvate kinase which can catalyze conversion of ADP to ATP was also significantly down-regulated in livers of rats exposed to 100 mg SCCPs/kg bm/d. In addition, expression of *Adcy10*, which encodes adenylate cyclase 10, was significantly increased in livers of rats exposed to 0.01 or 100 mg SCCPs/kg bm/d groups. Inhibition of the turnover of ATP-ADP-AMP would inevitably limit energy production.

4. Discussion

Due to the function of PPARα on lipid metabolism and peroxisome proliferation, and the structural similarity between SCCPs and natural ligands (fatty acids) for PPARα (Krey et al., 1997), it was speculated that SCCPs might activate PPARα and lead to adverse effects on metabolism in hepatocytes, however, no direct evidence of activation of PPARα by SCCPs has been reported previously. In the present study, this hypothesis was verified by use of a combination of metabolomics and transcriptomics and the results suggest two major modes of toxic action for SCCPs: (1) inhibition of energy metabolism and (2) activation of PPARα, and demonstrated possible effects of health due to chronic exposure to low-dose of SCCPs.

4.1. Evidences of SCCP-induced activation of PPARα

Results of this study suggest that SCCPs caused hepatotoxicity by activation of PPARα. PPARα is a transcription factor and a major regulator of hepatic lipid metabolism. Upon activation, PPARα forms a heterodimer with the retinoid X receptor (RXR) and then binds to a specific peroxisome proliferator response element (PPRE) in or around target genes. 16 genes regulated by PPARα (Golla et al., 2016; Rakhshandehroo et al., 2010; Zhang et al., 2018), including *Hadhb*, *Eci1*, *Decr2*, *Ech1*, *Ehhadh*, *Acaa1a*, *Acaa1b*, *Acot2*, *Fasn*, *Fads2*, *Cyp4a1*, *Elovl2*, *Elovl6*, *Lpin1*, *Lpin2* and *Me1*, were up-regulated after exposure to SCCPs (Figs. 4A and 5B), indicating that exposure to SCCPs activated the PPARα signaling pathway. Among them, 13 genes were involved in fatty acid metabolism, which suggests that oxidation, biosynthesis and elongation of fatty acids were stimulated. In addition, decreased Σfatty acids in livers of rats exposed to SCCPs further indicated the induction of fatty acid metabolism. In several toxicological studies of SCCPs on male rats, increased proliferation of peroxisomes, hepatocellular

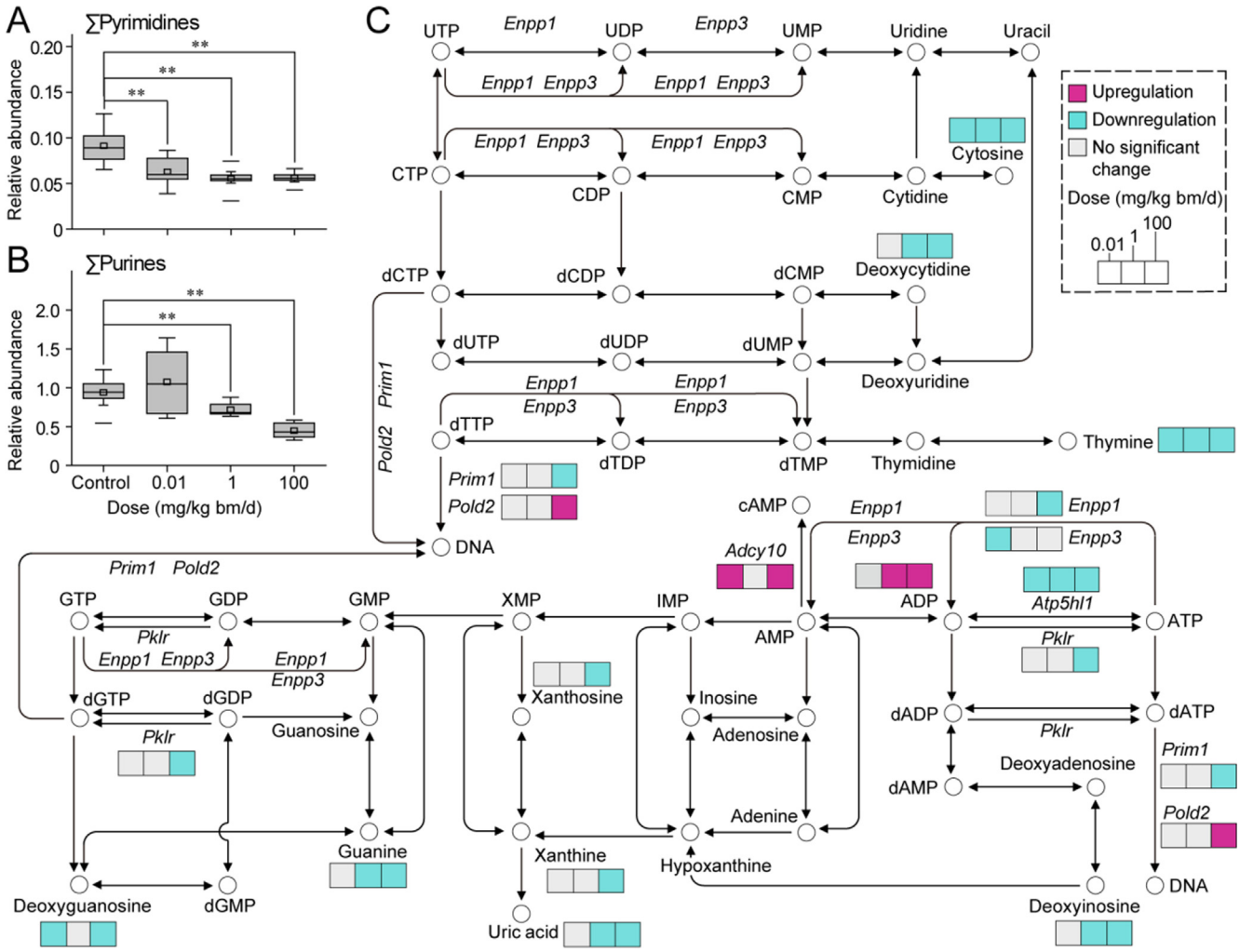

Fig. 6. Disorder of nucleotide metabolism in liver of SD rat after 28-day oral administration of SCCPs. (*A*) and (*B*) Total concentrations of pyrimidines (ΣPyrimidines) and purines (ΣPurines) in liver of unexposed (control) SD rat or three oral doses of SCCPs. (*C*) Most relevant metabolites and differentially expressed genes perturbed by SCCPs in nucleotide metabolism, **, $P < 0.01$.

carcinoma and greater liver weight were observed, all of which are consistent with activation of PPARα (Bucher et al., 1987; Nilsen et al., 1981; Wyatt et al., 1993). In the present study, greater liver weight was also observed at dose of SCCPs near the LOAEL (Fig. S2C). In addition, five genes (*Fbp2, Acot, Decr2, Hadhb, Hibch*) were up-regulated by a fold change of > 1.5 in mouse liver after exposure to three PPARα activators (Oshida et al., 2015), which verified the PPARα activation effect of SCCPs. Moreover, agonism of SCCPs towards the rat PPARα was confirmed by luciferase reporter gene assays. Exposure to SCCPs caused a dose-dependent increase in luciferase activity in rat PPARα-transfected kidney 293T cells, which was a more than 20% increase for the luciferase activity when exposed to doses of SCCPs > 1 μmol/L (Gong et al., 2019). These results demonstrated the transactivation potency of SCCPs towards rat PPARα.

4.2. SCCPs inhibit energy metabolism

Energy metabolism is the process by which ATP is generated via oxidative phosphorylation and glycolysis. In the present study, exposure to SCCPs inhibited energy production from oxidative phosphorylation, as determined by an increase in concentrations of ADP and lesser expression of *Atp5hl1*. Oxidative phosphorylation comprises respiratory chain complexes I to IV together with ATP synthase (complex V). Lesser expression of *Atp5hl1* might result in a deficit in ATP synthase. Moreover, exposure to SCCPs affected transfer of electrons in the respiratory chain. SCCPs blocked transfer of electrons in respiratory complex II (succinate dehydrogenase). This enzyme complex oxidizes succinate to fumarate and transfers electrons through three iron-sulfur clusters to ubiquinone, and thus participates in both the TCA cycle and the electron transport chain. In this study, concentrations of succinate, 2-oxoglutarate and malate were less in livers of rats exposed to SCCPs, compared to that in the control group (Fig. 5B), which indicated inhibition of the TCA cycle. The decreased levels of succinate and inhibition of the TCA cycle would inevitably decrease efficiency of electron transfer to ubiquinone. Alternatively, exposure to SCCPs might stimulate transfer of electrons in respiratory complex I (NADH: ubiquinone oxidoreductase) by accelerating oxidation of fatty acids through activation of the PPARα.

In rat hepatocytes, oxidative phosphorylation occurs in mitochondria. SCCPs inhibited oxidative phosphorylation implies that the mitochondrion is an important target of SCCPs. Mitochondrial dysfunction is likely a major mechanism of SCCPs induced liver toxicity (Porceddu et al., 2012). It was speculated that oxidative phosphorylation was suppressed partially to minimize ROS production. In the present study, elevation of GSSH in livers of rats exposed to all doses of SCCPs suggests that ROS-induced oxidative stress was significantly increased (Fig. 5B). As evidenced by up-regulation of *Pold2*, which encodes DNA polymerase delta subunit 2 (Fig. 6B), SCCPs may cause damage to DNA, and suppression of oxidative phosphorylation is a biochemical response to SCCP-induced DNA damage (Zhang et al., 2017).

Exposure to SCCPs inhibited glycolysis, which is another pathway for generation of ATP. Down-regulation of *Pklr* exposure to high dose SCCPs might decrease activity of pyruvate kinase and thus decrease generation of ATP via glycolysis (Fig. 5B). Because pyruvate kinase catalyzes the transphosphorylation of phohsphoenolpyruvate into pyruvate and ATP, which is the rate-limiting step of glycolysis. As a direct degradation product of pyruvate, concentration of L-lactate also exhibited a decreasing trend in livers of rats in two SCCP-treated groups compared with the control group. Also, activity of lactate dehydrogenase was also significantly decreased in blood of rats exposed to 1 mg SCCPs/kg bm/d (Fig. S2D), which further verified that SCCPs inhibited glycolysis. Lesser concentrations of glucose in livers of rats exposed to SCCPs might have resulted from suppression of gluconeogenesis, which is a major contributor to blood glucose homeostasis (Wang et al., 2018a). In the gluconeogenesis pathway, expression of *Fbp2* was significantly decreased in livers of rats exposed to 100 mg SCCPs/kg bm/d, compared with expression in the control rats (Fig. 5B). The enzyme encode by *Fbp2* can catalyze the conversion of fructose-1,6-bisphosphate to fructose 6-phosphate, which is the rate-limiting step in gluconeogenesis.

Inhibition of ATP-ADP-AMP turnover by SCCPs was characterized by the decreased expression levels of *Atp5hl1*, *pklr, Enpp1 and Enpp3* (Fig. 6C). Inhibited conversion of ATP to AMP and reduced concentrations of blood glucose might stimulate the activity of adenylate cyclase to maintain or increase concentrations of cAMP, which is a key second messenger molecule affecting multiple cellular processes in the liver. High concentrations of cAMP have been reported to increase glucose production by stimulating gluconeogenesis and glycogenolysis (Huang et al., 2013; Wahlang et al., 2018). In the present study, up-regulation of *Adcy10* was observed in livers of rats exposed to SCCPs (Fig. 6C). Inhibition of oxidative phosphorylation, glucose metabolism and ATP turnover, together with greater concentrations of ADP, suggest that exposure to SCCPs substantially inhibited energy metabolism in livers of rat. Consequently, the active transport of nutrients such as amino acids, glucose and nucleotides would be inevitably reduced. In the study, results of which are presented here, the concentrations of Σamino acids, Σpyrimidines and Σpurines were all remarkably reduced in the livers of rats exposed to the three doses of SCCPs (Figs. 5A, 6A and 6B). In an *in vitro* study, significant reductions in Na^+/K^+-ATPase activity and concentrations of ATP were observed in HepG2 cells exposed to SCCPs (Wang et al., 2018b).

4.3. Possible health effects of exposure to low-dose SCCPs

With their large and widespread use in industrial applications, SCCPs have been ubiquitously detected in environment and the human body at low doses. In the present study, it was found that SCCPs caused significant alterations in metabolism and energy conversion in the liver of SD rats even at environmentally relevant doses. Inhibition of energy metabolism resulted in alterations in active transport of amino acids, glucose and nucleotides and thus resulted in lesser concentrations of threonine, serine, methionine, asparagine, glutamine, thymine and cytosine in livers of rats exposed to all three doses of SCCPs (Figs. 5B and 6B), that might inhibit a series of biological reactions, including amino acid metabolism, nucleotide metabolism, protein biosynthesis, DNA replication and DNA repair, all of which would ultimately affect growth. Lower body mass gain has been observed in rats exposed to SCCPs at environmentally relevant doses. Moreover, pathophysiological analysis also indicated that exposure to SCCPs at environmentally relevant doses induced a considerable reduction in creatine kinase activity, which might results from inhibition of energy metabolism. Because livers of rats and human share similar mechanisms and pathways for energy metabolism, it was speculated that exposure to SCCPs at environmentally relevant doses would inhibit energy metabolism in human liver. In previous *in vitro* studies, it was observed that exposure to SCCPs at environmentally relevant doses resulted in lower concentrations of amino acids and nucleotides in human HepG2 hepatocytes (Geng et al., 2015; Wang et al., 2018b). Inhibition of energy metabolism in the human liver might cause nutrient deficiency and loss of body mass.

Although activation of PPARα by SCCPs was observed at high dose in this study, an acceleration of fatty acid metabolism, which mainly resulted from the SCCP-induced activation of a small amount of PPARα, was caused by exposure to SCCPs at environmentally relevant doses. Rats and humans share similar tissue distribution profiles for expression of PPARα (Mukherjee et al., 1994). While, because expression of mRNA for PPARα was only at low levels in human liver and humans are less sensitive than rodents to effect of peroxisome proliferation (Bility et al., 2004; Palmer et al., 1998), the importance of PPARα in human liver has been questioned. However, results of recent studies using more advanced methodologies revealed similar PPARα levels in some people to those observed in mice and rats (Walgren et al., 2000), which provided evidence against this hypothesis. Therefore, SCCP-induced hepatotoxicity that occurs via interactions with PPARα should be carefully evaluated in vulnerable subpopulations of humans.

The balance of ω-6 and ω-3 fatty acids in an organism is essential for normal growth and development, and the ω-6/ω-3 ratio plays an important role in tumorigenesis (Xia et al., 2006, 2005). The dose-dependent increase in ω-6/ω-3 ratio suggests that rats exposed to SCCPs had a high risk of developing tumors and cancer. Results of a 2-year study in which rats were exposed to SCCPs indicate the potential carcinogenicity (Bucher et al., 1987), and SCCPs have been classified, in 1990, by the International Agency for Research on Cancer (IARC) as a Group 2B carcinogen, that is possibly carcinogenic to humans (IARC, 1990).

5. Conclusions

Exposure of rats to SCCPs was shown to cause hepatotoxicity at environmentally relevant dosages. Changes to metabolism of lipids, amino acids and nucleotides in livers of rats after low-dose exposure to SCCPs were linked to transcriptomic changes, and might partly explain the results of histological examinations, blood glucose and body mass changes in rat exposed to SCCPs at the high dose. SCCPs might act as PPARα agonists and up-regulating relevant expression of genes, stimulating *β*-oxidation of unsaturated fatty acids (Geng et al., 2015) as well as peroxisome proliferation in liver of rodents (Wyatt et al., 1993). Exposure to SCCPs suppresses oxidative phosphorylation, glycolysis, gluconeogenesis and ATP-ADP-AMP turnover, and thus induces amino acid and nucleotide deficiencies in livers of rat. Significant SCCP-induced inhibition of energy metabolism occurs at environmentally relevant doses, which suggests that SCCPs exhibit significant effects on metabolism. Collectively, results of the current study provide understanding for the molecular mechanisms of hepatotoxicity and adverse health effects caused by exposure to SCCPs.

Limitations and future directions

In this study, omic techniques were found to be powerful tools to observe global biological changes following exposures to SCCPs, even at low doses. Results of this study raise importance regarding the role of PPAR*α* and energy metabolism to SCCPs induced hepatotoxicity in SD rat. However, this study has some limitations. Thus, to further verify agonism of SCCPs to the PPARα, expression/knockdown experiments should be performed to make this conclusion more convincing. To verify the inhibition of energy metabolism caused by SCCPs, a detailed evaluation of mitochondrial respiration and glycolysis, the two major energy-producing pathways in the cell, will be performed. In particular, in view of the fact that rat and human livers share similar mechanisms for energy metabolism and similar PPARα tissue expression profiles, work is ongoing based on a human hepatic cell-line to explore the possible health effects induced by SCCPs. In our future studies, system verification will be performed to provide a better understanding for the mechanisms of SCCPs induced liver toxicity.

Declaration of Competing Interest

The authors declare that they have no known competing financial interests or personal relationships that could have appeared to influence the work reported in this paper.

Acknowledgments

This work was financially supported by National Basic Research Program of China (grant no. 2015CB453100) and National Natural Science Foundation of China (grant nos. 21607152, 21277141, 21337002 and 91543201).

Appendix A. Supplementary material

Gene expression analysis; LC-MS-based metabonomic analysis; Determination of TELI and MELI; General pathophysiological results; Detail information of 63 DEGs and 118 DMs; Results of pathophysiological tests and RT-PCR validation were offered in Supplemental Material. Supplementary data to this article can be found online at https://doi.org/10.1016/j.envint.2019.105231.

References

Ali, T.E.-S., Legler, J., 2010. Overview of the mammalian and environmental toxicity of chlorinated paraffins. In: Boer, J. (Ed.), Chlorinated Paraffins. Springer, Berlin, Heidelberg, pp. 135–154.

Bility, M.T., Thompson, J.T., McKee, R.H., David, R.M., Butala, J.H., Vanden Heuvel, J.P., Peters, J.M., 2004. Activation of mouse and human peroxisome proliferator-activated receptors (PPARs) by phthalate monoesters. Toxicol. Sci. 82, 170–182. https://doi.org/10.1093/toxsci/kfh253.

Bucher, J.R., Alison, R.H., Montgomery, C.A., Huff, J., Haseman, J.K., Farnell, D., Thompson, R., Prejean, J.D., 1987. Comparative toxicity and carcinogenicity of two chlorinated paraffins in F344/N rats and B6C3F1 mice. Fundam. Appl. Toxicol. 9, 454–468. https://doi.org/10.1093/toxsci/9.3.454.

Burri, L., Thoresen, G.H., Berge, R.K., 2010. The role of PPAR activation in liver and muscle. PPAR Res. 2010, 542359. https://doi.org/10.1155/2010/542359.

Buryskova, B., Blaha, L., Vrskova, D., Simkova, K., Marsalek, B., 2006. Sublethal toxic effects and induction of glutathione S-transferase by short chain chlorinated paraffins (SCCPs) and C-12 alkane (dodecane) in Xenopus laevis frog embryos. Acta Vet. Brno 75, 115–122. https://doi.org/10.2754/avb200675010115.

International Agency for Research on Cancer (IARC), 1990. Some Flame Retardants and Textile Chemicals, and Exposures in the Textile Manufacturing Industry. IARC Monographs on the Evaluation of Carcinogenic Risks To Humans, Lyon, France, pp. 55–72.

Cao, Y., Harada, K.H., Liu, W.Y., Yan, J.X., Zhao, C., Niisoe, T., Adachi, A., Fujii, Y., Nouda, C., Takasuga, T., Koizumi, A., 2015. Short-chain chlorinated paraffins in cooking oil and related products from China. Chemosphere 138, 104–111. https://doi.org/10.1016/j.chemosphere.2015.05.063.

Cao, Y., Harada, K.H., Hitomi, T., Niisoe, T., Wang, P., Shi, Y., Yang, H.R., Takasuga, T., Koizumi, A., 2017. Lactational exposure to short-chain chlorinated paraffins in China, Korea, and Japan. Chemosphere 173, 43–48. https://doi.org/10.1016/j.chemosphere.2016.12.078.

Chen, H., Lam, J.C.W., Zhu, M.S., Wang, F., Zhou, W., Du, B.B., Zeng, L.X., Zeng, E.Y., 2018. Combined effects of dust and dietary exposure of occupational workers and local residents to short- and medium-chain chlorinated paraffins in a mega e-waste recycling industrial park in south China. Environ. Sci. Technol. 52, 11510–11519. https://doi.org/10.1021/acs.est.8b02625.

Ehara, T., Kamei, Y., Yuan, X., Takahashi, M., Kanai, S., Tamura, E., Tsujimoto, K., Tamiya, T., Nakagawa, Y., Shimano, H., Takai-Igarashi, T., Hatada, I., Suganami, T., Hashimoto, K., Ogawa, Y., 2015. Ligand-activated PPARα-dependent DNA demethylation regulates the fatty acid β-oxidation genes in the postnatal liver. Diabetes 64, 775–784. https://doi.org/10.2337/db14-0158.

Fiedler, H., 2010. Short-chain chlorinated paraffins: production, use and international regulations. In: Boer, J. (Ed.), Chlorinated Paraffins. Springer, Berlin, Heidelberg, pp. 1–40.

Friden, U.E., McLachlan, M.S., Berger, U., 2011. Chlorinated paraffins in indoor air and dust: concentrations, congener patterns, and human exposure. Environ. Int. 37, 1169–1174. https://doi.org/10.1016/j.envint.2011.04.002.

Gao, W., Cao, D.D., Wang, Y.J., Wu, J., Wang, Y., Wang, Y.W., Jiang, G.B., 2017. External exposure to short- and medium-chain chlorinated paraffins for the general population in Beijing, China. Environ. Sci. Technol. 52, 32–39. https://doi.org/10.1021/acs.est.7b04657.

Gao, Y., Zhang, H.J., Chen, J.P., Zhang, Q., Tian, Y.Z., Qi, P.P., Yu, Y.Z., 2011. Optimized cleanup method for the determination of short chain polychlorinated n-alkanes in sediments by high resolution gas chromatography/electron capture negative ion–low resolution mass spectrometry. Anal. Chim. Acta 703, 187–193. https://doi.org/10.1016/j.aca.2011.07.041.

Geng, N.B., Zhang, H.J., Zhang, B.Q., Wu, P., Wang, F.D., Yu, Z.K., Chen, J.P., 2015. Effects of short-chain chlorinated paraffins exposure on the viability and metabolism of human hepatoma HepG2 cells. Environ. Sci. Technol. 49, 3076–3083. https://doi.org/10.1021/es505802x.

Gluge, J., Wang, Z.Y., Bogdal, C., Scheringer, M., Hungerbuhler, K., 2016. Global production, use, and emission volumes of short-chain chlorinated paraffins - a minimum scenario. Sci. Total Environ. 573, 1132–1146. https://doi.org/10.1016/j.scitotenv.2016.08.105.

Golla, U., Joseph, D., Tomar, R.S., 2016. Combined transcriptomics and chemical-genetics reveal molecular mode of action of valproic acid, an anticancer molecule using budding yeast model. Sci. Rep. 6, 35322. https://doi.org/10.1038/srep35322.

Gong, Y.F., Zhang, H.J., Geng, N.B., Xing, L.G., Fan, J.F., Luo, Y., Song, X.Y., Ren, X.Q., Wang, F.D., Chen, J.P., 2018. Short-chain chlorinated paraffins (SCCPs) induced thyroid disruption by enhancement of hepatic thyroid hormone influx and degradation in male Sprague Dawley rats. Sci. Total Environ. 625, 657–666. https://doi.org/10.1016/j.scitotenv.2017.12.251.

Gong, Y.F., Zhang, H.J., Geng, N.B., Ren, X.Q., Giesy, J.P., Luo, Y., Xing, L.G., Wu, P., Yu, Z.K., Chen, J.P., 2019. Short-chain chlorinated paraffins (SCCPs) disrupt hepatic fatty acid metabolism in liver of male rat via interacting with peroxisome proliferator-activated receptor α (PPARα). Ecotox. Environ. Safe 2019 (181), 164–171. https://doi.org/10.1016/j.ecoenv.2019.06.003.

Hüttig, J., Oehme, M., 2005. Presence of chlorinated paraffins in sediments from the North and Baltic Seas. Arch. Environ. Contam. Toxicol. 49, 449–456. https://doi.org/10.1007/s00244-005-7024-7.

Huang, P.L., Chi, C.W., Liu, T.Y., 2013. Areca nut procyanidins ameliorate streptozocin-induced hyperglycemia by regulating gluconeogenesis. Food Chem. Toxicol. 55, 137–143. https://doi.org/10.1016/j.fct.2012.12.057.

Krey, G., Braissant, O., L'Horset, F., Kalkhoven, E., Perroud, M., Parker, M.G., Wahli, W., 1997. Fatty acids, eicosanoids, and hypolipidemic agents identified as ligands of peroxisome proliferator-activated receptors by coactivator-dependent receptor ligand assay. Mol. Endocrinol. 11, 779–791. https://doi.org/10.1210/mend.11.6.0007.

Li, H.J., Fu, J.J., Zhang, A.Q., Zhang, Q.H., Wang, Y.W., 2016. Occurrence, bioaccumulation and long-range transport of short-chain chlorinated paraffins on the Fildes Peninsula at King George Island. Antarctica. Environ. Int. 94, 408–414. https://doi.org/10.1016/j.envint.2016.05.005.

Li, T., Wan, Y., Gao, S.X., Wang, B.L., Hu, J.Y., 2017. High-throughput determination and characterization of short-, medium-, and long-chain chlorinated paraffins in human blood. Environ. Sci. Technol. 51, 3346–3354. https://doi.org/10.1021/acs.est.6b05149.

Liu, L.H., Li, Y.F., Coelhan, M., Chan, H.M., Ma, W.L., Liu, L.Y., 2016. Relative developmental toxicity of short-chain chlorinated paraffins in Zebrafish (Danio rerio) embryos. Environ. Pollut. 219, 1122–1130. https://doi.org/10.1016/j.envpol.2016.09.016.

Mukherjee, R., Jow, L., Noonan, D., McDonnell, D.P., 1994. Human and rat peroxisome proliferator activated receptors (PPARs) demonstrate similar tissue distribution but different responsiveness to PPAR activators. J. Steroid Biochem. 51, 157–166. https://doi.org/10.1016/0960-0760(94)90089-2.

Nielsen, E., Ladefoged, O. (Eds.), 2013. Evaluation of Health hazards by Exposure to Chlorinated Paraffins and Proposal of A Health-Based Quality Criterion for Ambient Air. The Danish Environmental Protection Agency, Copenhagen.

Nilsen, O.G., Toftgard, R., Glaumann, H., 1981. Effects of chlorinated paraffins on rat liver microsomal activities and morphology. Arch. Toxicol. 49, 1–13. https://doi.org/10.1007/BF00352066.

Oshida, K., Vasani, N., Thomas, R.S., Applegate, D., Rosen, M., Abbott, B., Lau, C., Guo, G., Aleksunes, L.M., Klaassen, C., Corton, J.C., 2015. Identification of modulators of the nuclear receptor peroxisome proliferator-activated receptor alpha (PPARalpha) in a mouse liver gene expression compendium. PLoS ONE 10, e0112655. https://doi.org/10.1371/journal.pone.0112655.

Palmer, C.N.A., Hsu, M.-H., Griffin, K.J., Raucy, J.L., Johnson, E.F., 1998. Peroxisome proliferator activated receptor-α expression in human liver. Mol. Pharmacol. 53, 14–22. https://doi.org/10.1124/mol.53.1.14.

Porceddu, M., Buron, N., Roussel, C., Labbe, G., Fromenty, B., Borgne-Sanchez, A., 2012. Prediction of liver injury induced by chemicals in human with a multiparametric assay on isolated mouse liver mitochondria. Toxicol. Sci. 129, 332–345. https://doi.org/10.1093/toxsci/KFS197.

Rakhshandehroo, M., Knoch, B., Muller, M., Kersten, S., 2010. Peroxisome proliferator-activated receptor alpha target genes. PPAR Res. 2010, 612089. https://doi.org/10.1155/2010/612089.

Shi, L.M., Gao, Y., Zhang, H.J., Geng, N.B., Xu, J.Z., Zhan, F.Q., Ni, Y.W., Hou, X.H., Chen, J.P., 2017. Concentrations of short- and medium-chain chlorinated paraffins in indoor dusts from malls in china: Implications for human exposure. Chemosphere 172, 103–110. https://doi.org/10.1016/j.chemosphere.2016.12.150.

Shi, L.M., Reid, L.H., Jones, W.D., Shippy, R., Warrington, J.A., Baker, S.C., et al., 2006. The microarray quality control (maqc) project shows inter- and intraplatform reproducibility of gene expression measurements. Nat. Biotechnol. 24, 1151–1161. https://doi.org/10.1038/nbt1239.

Spivey, A., 2004. Systems biology: the big picture. Environ. Health Perspect. 112, A938–A943. https://doi.org/10.1289/ehp.112-a938.

Thomas, G.O., Farrar, D., Braekevelt, E., Stern, G., Kalantzi, O.I., Martin, F.L., Jones, K., 2006. Short and medium chain length chlorinated paraffins in UK human milk fat. Environ. Int. 32, 34–40. https://doi.org/10.1016/j.envint.2005.04.006.

United Nations Environment Programme (UNEP), 2011. Revised draft risk profile: Short-chained chlorinated paraffins. UNEP/POPS/POPRC.6/11/Rev.1, Geneva, 22–23. Available at: http://chm.pops.int/Default.aspx?tabid=2301.

Vandenberg, L.N., Colborn, T., Hayes, T.B., Heindel, J.J., Jacobs, D.R., Le, D.-H., Shioda, T., Soto, A.M., vom Saal, F.S., Welshons, W.V., Zoeller, R.T., Myers, J.P., 2012.

Hormones and endocrine-disrupting chemicals: Low-dose effects and nonmonotonic dose responses. Endocr. Rev. 33, 378–455. https://doi.org/10.1210/er.2011-1050.

Wahlang, B., McClain, C., Barve, S., Gobejishvili, L., 2018. Role of cAMP and phosphodiesterase signaling in liver health and disease. Cell. Signal. 49, 105–115. https://doi.org/10.1016/j.cellsig.2018.06.005.

Walgren, J.E., Kurtz, D.T., McMillan, J.M., 2000. Expression of PPAR(alpha) in human hepatocytes and activation by trichloroacetate and dichloroacetate. Res. Commun. Mol. Pathol. Pharmacol. 108, 116–132.

Wang, B., Smyl, C., Chen, C.-Y., Li, X.-Y., Huang, W., Zhang, H.-M., Pai, V.J., Kang, J.X., 2018a. Suppression of postprandial blood glucose fluctuations by a low-carbohydrate, high-protein, and high-omega-3 diet via inhibition of gluconeogenesis. Int. J. Mol. Sci. 19, 1823. https://doi.org/10.3390/ijms19071823.

Wang, F.D., Zhang, H.J., Geng, N.B., Ren, X.Q., Zhang, B.Q., Gong, Y.F., Chen, J.P., 2018b. A metabolomics strategy to assess the combined toxicity of polycyclic aromatic hydrocarbons (PAHs) and short-chain chlorinated paraffins (SCCPs). Environ. Pollut. 234, 572–580. https://doi.org/10.1016/j.envpol.2017.11.073.

Wei, G.L., Liang, X.L., Li, D.Q., Zhuo, M.N., Zhang, S.Y., Huang, Q.X., Liao, Y.S., Xie, Z.Y., Guo, T.L., Yuan, Z.J., 2016. Occurrence, fate and ecological risk of chlorinated paraffins in Asia: a review. Environ. Int. 92–93, 373–387. https://doi.org/10.1016/j.envint.2016.04.002.

Wyatt, I., Coutss, C.T., Elcombe, C.R., 1993. The effect of chlorinated paraffins on hepatic enzymes and thyroid hormones. Toxicology 77, 81–90. https://doi.org/10.1016/0300-483X(93)90139-J.

Xia, D., Gao, L.R., Zheng, M.H., Li, J.G., Zhang, L., Wu, Y.N., Tian, Q.C., Huang, H.T., Qiao, L., 2017. Human exposure to short- and medium-chain chlorinated paraffins via mothers' milk in chinese urban population. Environ. Sci. Technol. 51, 608–615. https://doi.org/10.1021/acs.est.6b04246.

Xia, S.H., Lu, Y., Wang, J.D., He, C.W., Hong, S., Serhan, C.N., Kang, J.X., 2006. Melanoma growth is reduced in fat-1 transgenic mice: Impact of omega-6/omega-3 essential fatty acids. Proc. Natl. Acad. Sci. USA 103, 12499–12504. https://doi.org/10.1073/pnas.0605394103.

Xia, S.H., Wang, J.D., Kang, J.X., 2005. Decreased n-6/n-3 fatty acid ratio reduces the invasive potential of human lung cancer cells by downregulation of cell adhesion/invasion-related genes. Carcinogenesis 26, 779–784. https://doi.org/10.1093/carcin/bgi019.

Zhang, C., Skamagki, M., Liu, Z., Ananthanarayanan, A., Zhao, R., Li, H., Kim, K., 2017. Biological significance of the suppression of oxidative phosphorylation in induced pluripotent stem cells. Cell Rep. 21, 2058–2065. https://doi.org/10.1016/j.celrep.2017.10.098.

Zhang, Q., Wang, J.H., Zhu, J.Q., Liu, J., Zhang, J.Y., Zhao, M.R., 2016. Assessment of the endocrine-disrupting effects of short-chain chlorinated paraffins in in vitro models. Environ. Int. 94, 43–50. https://doi.org/10.1016/j.envint.2016.05.007.

Zhang, W.L., Zhong, W., Sun, Q., Sun, X.G., Zhou, Z.X., 2018. Adipose-specific lipin1 overexpression in mice protects against alcohol-induced liver injury. Sci. Rep. 8, 408. https://doi.org/10.1038/s41598-017-18837-2.

Supplemental Material

Integration of Metabolomics and Transcriptomics reveals Short-chain Chlorinated Paraffin-induced Hepatotoxicity in Male Sprague-Dawley Rat

Ningbo Geng, Xiaoqian Ren, Yufeng Gong, Haijun Zhang, Feidi Wang, Liguo Xing, Rong Cao, Jiazhi Xu,Yuan Gao, John P. Giesy, and Jiping Chen

Table of Contents

1. Gene expression analysis. Liver were collected from SD rats after 28-d exposure to SCCPs. The samples were preserved in liquid nitrogen until gene expression analysis. Approximately 100 mg of liver was pulverized using a mortar with liquid nitrogen and further processed for total RNA following the standard instructions. Total RNA was extracted and purified using mirVana™ miRNA Isolation Kit (Cat$^{\#}$AM1561, Ambion, Austin, TX, US). After extraction, Agilent Bioanalyzer 2100 (Agilent technologies, Santa Clara, CA, US) was used to evaluate the RNA quality and quantity.

Eight DEGs were selected for quantitative RT-PCR validation. Oligonucleotide primers were designed for the specific amplification of *Cdk1*, *Ednra*, *Pfkfb1*, *Slpi*, *Herpud1*, *Acaa1b*, *Alas1*, and *Acot2* by using Primer Premier 5.0 software (PREMIER Biosoft Int., Palo Alto, CA, USA) with the sequences for rat available from the GenBank database (Table S4). Real-time PCRs were carried out by ABI power SYBR green PCR master mix (ABI, USA). Amplification was performed in an 7900 HT Sequence Detection System (ABI, USA), with the following cycling conditions: 50 °C for 2 min and 95 °C for 10 min, followed by 40 cycles at 95 °C for 15 s and 60 °C for 60 s. Melt curve analysis was performed to confirm the PCR specificity. For each analysis, the relative target gene mRNA expression levels were normalized to the geometric mean of β-actin expression levels, according to the formula $2^{-\triangle\triangle Ct}$ and plotted on a logarithmic scale (Peters et al. 1997). As shown in Table S4, all the eight comparisons were validated by qRT–PCR. The overall consistency between qRT–PCR and microarray results suggested the reliability of microarray to accurately quantify transcriptome wide gene expression.

2. LC-MS-based metabonomic analysis. Samples of liver tissue (100 mg) were mixed with 1 mL of H_2O and homogenized using a high-speed homogenizer. The homogenate was ultra-sonicated for 5 min in an ice water bath. The homogenated sample was freeze-dried and subsequently extracted with 0.5 mL of methanol/water (4:1, v/v).The mixed solution was vortexed for 30 min, and centrifuged at 13,000 × g for 20 min at 8 °C. Finally, the supernatant was filtered by an organic phase filter and transferred to a vial for metabolite analysis. Six internal standards were spiked into the vial for the quality control of sample preparation and instrumental analysis.

A pseudotargeted approach was used for the metabolomic analysis. In brief, the extracts from liver samples was first used for untargeted analysis, then used for targeted analysis in multiple reaction monitoring (MRM) mode. The MRM ion pairs

were acquired through untargeted analysis in auto MS/MS mode for the extracts. MRM ion pairs selection including precursor ion alignment, auto MS/MS spectra data extraction and characteristic product ion selection. After execution, the detected metabolite ions with information about the precursor ion, product ions, retention time, and collision energy were exported to a spreadsheet for scheduled MRM detection. Finally, six hundred eighty-eight ion pairs were analyzed in the mode of ESI^+ and ESI^- mode.

The untargeted analysis was performed on the Agilent UPLC/Q-TOF MS system operated in both positive and negative electrospray ionization modes (ESI^+/ ESI^-). Column temperature and automatic sampler temperature were set at 50 °C and 8 °C, respectively. The injection volume was 5 μL. In ESI^+ mode, the chromatography separation was carried out on a Waters Acquity BEH C8 column (100 mm × 2.1 mm, 1.7 μm). The mobile phase A was 0.1% (v/v) formic acid in water, and the phase B was 0.1% (v/v) formic acid in acetonitrile. The flow rate was 0.35 mL/min, and the gradient elution was as follows: (time, %B): 0 min, 10%; 3 min, 40%; 15 min, 100%, and maintained for 5 min; 20.1 min, 10%, and re-equilibrated for 2.9 min before the next analysis. The mass spectrometer was operated with a capillary voltage of 3500 V, fragment or voltage of 175 V, skimmer voltage of 65 V, nebulizer gas (N_2) pressure at 35 psi, drying gas (N_2) flow rate of 8 L/min, and a temperature of 350 °C. The auto-MS/MS mode was performed on the three most intense precursors were chosen within one full scan cycle (0.25 s). The precursor ion scan range was set with m/z 50−1000 and a MS/MS scan range of m/z 30−1000. The collision energies were set base on the formula CE = 5 × (m/z)/100 + 3, and all samples were analyzed to obtain abundant and complementary product ion information.

In ESI^- mode, an Acquity UPLC HSS T3 column (2.1 mm × 100 mm × 1.8 μm, Waters, USA) was used for the chromatographic separation. Water and methanol both containing 5 mmol/L ammonium bicarbonate were used as mobile phases A and B, respectively. The flow rate was also 0.35 mL/min, and the gradient elution was as follows (time, %B): 0 min, 2%; 3 min, 42%; 12 min, 100%, and maintained for 4 min; 16.1 min, 2%, and re-equilibrated for 3.9 min. The mass spectrometer was operated with a capillary voltage of 3500 V, fragment or voltage of 175 V, skimmer voltage of 65 V, nebulizer gas (N_2) pressure at 35 psi, drying gas (N_2) flow rate of 8 L/min, and a temperature of 350 °C. The auto-MS/MS mode was performed on the three most intense precursors were chosen within one full scan cycle (0.25 s) with a precursor ion

scan range of m/z 50−1000 and a tandem mass scan range of m/z 30−1000. The collision energies were set base on the formula CE = 5 × (m/z)/100 + 3, and all samples were analyzed to obtain abundant and complementary product ion information.

Raw data obtained from Q-TOF MS were analyzed using Mass Hunter software 4.0 and Mass Profiler Professional 2.2 (MPP), both from Agilent. Metabolite identification was performed by matching the obtained accurate m/z values and theoretical m/z values with a mass accuracy window of 10 ppm in free available databases Human Metabolome Database (HMDB) and Agilent Metabolomics Database (METLIN).When available, standards were used to confirm metabolite identification. MultiQuant software 3.0 (AB SCIEX) was used for data processing of the Q-Trap MS data. After the peak alignment and the removal of the missing values, ion peak areas across ESI^+ and ESI^- modes were normalized to internal standards and then merged into one data set. Then each peak area in the merged data set was normalized to the total peak area.

To ensure data quality for metabolic profiling, pooled quality control (QC) samples were prepared by mixing all of the samples, and insert into the analytical sequence after each set of 10 samples. Eight replicates of the QC samples were obtained, the relative standard deviation (RSD) for the concentration of each metabolite was calculated from the obtained data of QC samples, and the results are shown in Figure S4. 77% of the metabolites detected had an RSD of < 30%. Principal component analysis (PCA) revealed that the scores of all QC samples along the first component fell within the confidence interval corresponding to two standard deviations (SD). The statistical results for the QC samples indicated satisfactory stability and repeatability of the sequencing analysis of targeted metabolites.

3. Determination of TELI and MELI. To quantify the transcriptional effect level induced by SCCPs exposure, TELI was used to convert the information-rich toxicogenomic data into an integrated endpoint, which can reflected the overall transcriptional alteration (Gou and Gu 2011). First, the transcriptional change (TC_i) of each gene in a sample was calculated according to equation 1:

$$TC_i = e^{|\ln(A_{t,i})|} - e^{|\ln(A_{t,c,i})|} \quad (1)$$

here $A_{t,i}$is the ratio of the relative abundance of a single gene (i) in exposure group to the mean relative abundance of this gene in the control group, and $A_{t,c,i}$ is the

relative transcriptional change of the control group, which is definited as 1. Then the transcriptional change of single gene of a sample was then summarized as accumulated transcriptional change of all *m* detected genes of this sample following equation 2: absolute transcriptional alteration without distinguishing decrease or increase of transcriptional levels are considered.

$$\mathrm{TELI} = (\sum_{i=1}^{i=m} \mathrm{TC}_i)/m \quad (2)$$

Similarly, metabolic responses related to exposure time were aggregated to the MELI to quantitatively assess the metabolic disturbance induced by SCCPs. MELI combine the abundant data information into an integrated endpoint to reveal the overall metabolic change after SCCPs exposure without distinguishing decrease or increase of metabolic levels (Riedl et al. 2015). First, the metabolic change (MC_i) of each metabolite in a sample was calculated according to the following equation:

$$\mathrm{MC}_i = e^{|\ln(A_{m,i})|} - e^{|\ln(A_{m,c,i})|} \quad (3)$$

where $A_{m,i}$ is the ratio between the abundance of a single metabolite (i) to the mean abundance of this metabolite in the control group, and $A_{m,c,i}$ is the relative metabolic change of the control group, which is definited as 1. The metabolic changes of each metabolite in a sample were then summarized as MELI to describe the change of all *n* quantified metabolites according to equation 4:

$$\mathrm{MELI} = (\sum_{i=1}^{i=n} \mathrm{TC}_i)/n \quad (4)$$

4. General pathophysiological results. A series of pathophysiological examinations of male SD rats exposed to SCCPs, including body mass, liver coefficient, liver morphometry, and clinical biochemical parameters were determined. The contents of SCCPs in livers of SD rats were analyzed after 28 d of oral administration (Figure S2A). SCCPs were not detected in livers of SD rats in the control or low-dose (MDL = 0.29 μg/g wet weight) groups. Mean concentrations of SCCPs were 0.68 and 2.4 mg/kg wet weight in livers of rats in the middle- and high-dose groups, respectively. Lower body mass gain was observed for rats exposed to all doses of SCCPs, but only male rats exposed to the high-dose of SCCPs exhibited markedly decreased (Student's *t*-test, $P < 0.05$) in body mass, compared to that for the control group (Figure S2B). Histological examinations of liver tissues did not reveal any treatment-related effects after 28 d of exposure to SCCPs. Liver coefficient was obtained from liver-to-body mass ratio and significantly higher liver coefficients were observed in rats exposed to high-dose SCCPs than in the controls (Figure S2C). Exposure to the low-dose SCCPs

for 28 d caused 0.4-fold, 0.5-fold, 0.5-fold and 0.3-fold decreases in lymphocyte count, highly fluorescent reticulocyte count, lactate dehydrogenase activity and creatine kinase activity, respectively (Figures S2D and E). A significant decrease in highly fluorescent reticulocyte count was also observed in the high-dose group. However, exposure to the low-dose of SCCPs did not cause significant effects on any clinical biochemical parameters compared with the control group (Tables S1–3).

Table S1. Hematological parameters of SD rats in the control and SCCPs-treated groups (*n*= 10, mean ± standard error).

Characters	Dose (mg/kg bm/d)			
	0	0.01	1	100
WBC (10^9/L)	17.4 ± 5.5	15.9 ± 4.0	10.7 ± 2.4**	14.5 ± 3.7
RBC (10^{12}/L)	8.5 ± 0.3	8.1 ± 0.3	8.4 ± 0.5	8.3 ± 0.5
HGB (g/L)	159.0 ± 6.0	156.0 ± 5.0	160.0 ± 8.0	154.0 ± 7.0
HCT (%)	48.9 ± 1.9	47.5 ± 1.8	48.2 ± 2.1	47.0 ± 2.0
MCV (fL)	57.8 ± 1.7	58.4 ± 2.5	57.5 ± 2.1	56.8 ± 2.5
MCH (pg)	18.8 ± 0.5	19.1 ± 0.8	19.0 ± 0.7	18.6 ± 0.6
MCHC (g/L)	326.0 ± 3.0	328.0 ± 3.0	331.0 ± 3.0*	328.0 ± 5.0
PLT (10^9/L)	1164.0 ± 94.0	1092.0 ± 127.0	1117.0 ± 146.0	1197.0 ± 170.0
PCT	1.0 ± 0.06	0.9 ± 0.1	0.9 ± 0.1	1.0 ± 0.1
MPV	8.7 ± 0.3	8.5 ± 0.2	8.3 ± 0.4	8.4 ± 0.5
PDW	10.4 ± 0.4	10.0 ± 0.4	9.7 ± 0.6*	10.0 ± 0.6
RET (%)	4.2 ± 0.6	3.9 ± 0.6	3.6 ± 0.6	3.3 ± 0.8*
LYMPH (%)	86.3 ± 3.9	85.3 ± 3.8	80.9 ± 3.1**	86.3 ± 3.1
MONO (%)	2.7 ± 0.6	3.2 ± 0.8	3.3 ± 1.0	3.5 ± 0.5
NEUT (%)	10.5 ± 3.8	10.9 ± 3.1	15.2 ± 2.7**	9.7 ± 3.2
EO (%)	0.4 ± 0.2	0.5 ± 0.3	0.6 ± 0.3	0.4 ± 0.2
BASO (%)	0.1 ± 0.1	0.1± 0.0	0.1 ± 0.0	0.1 ± 0.0
LYMPH (10^9/L)	15.1 ± 5.0	13.7 ± 3.9	8.7 ± 2.1**	12.5 ± 3.4
MONO (10^9/L)	0.5 ± 0.2	0.5 ± 0.09	0.3 ± 0.08	0.5 ± 0.2
NEUT (10^9/L)	1.8 ± 0.6	1.7 ± 0.4	1.6 ± 0.4	1.4 ± 0.4
EO (10^9/L)	0.08 ± 0.06	0.07 ± 0.05	0.06 ± 0.03	0.06 ± 0.03
BASO (10^9/L)	0.01 ± 0.01	0.01 ± 0.00	0.01 ± 0.00	0.01 ± 0.01
RDW_CV	17.5 ± 1.1	16.4 ± 1.1	16.9 ± 1.3	17.5 ± 1.7
RDW_SD	31.8 ± 1.2	30.7 ± 0.9	30.7 ± 1.1	31.7 ± 1.7
P_LCR	16.6 ± 1.9	15.1 ± 1.8	13.8 ± 2.7*	14.7 ± 3.2
RET	352.4 ± 44.7	320.4 ± 56.7	302.3 ± 62.1	275.3 ± 68.4*
IRF	46.5 ± 3.6	44.3 ± 5.3	39.4 ± 5.5*	38.5 ± 8.1*
LFR (10^9/L)	53.5 ± 3.6	55.7 ± 5.3	60.6 ± 5.5*	61.5 ± 8.1*
MFR (%)	23.3 ± 2.9	24.6 ± 2.9	25.7 ± 3.3	23.9 ± 3.8
HFR (%)	23.2 ± 4.3	19.7 ± 4.3	13.7 ± 3.6**	14.6 ± 5.4**
HFR (10^9/L)	82.5 ± 21.2	64.3 ± 22.5	41.6 ± 14.4**	42.9 ± 23.6**

Note: WBC (white blood cell count), RBC (red blood cell count), HGB (hemoglobin concentration), HCT (hematocrits), MCV (mean corpuscular volume), MCH (mean corpuscular hemoglobin), MCHC (mean corpuscular hemoglobin concentration), PLT (platelet count), PCT (plateletcrit), MPV (mean platelet volume), PDW (platelet distribution width), RET (reticulocyte count), LYMPH (lymphocyte count)，MONO (Monocyte count)，NEUT (neutrophil count), EO (eosinophil count), BASO (basophilia count), RDW (red cell distribution width), P_LCR (platelet-large cell ratio), IRF (immature reticulocyte fraction), LFR (low fluorescent reticulocyte), MFR (middle fluorescent reticulocyte), HFR (high fluorescent reticulocyte).*, $P < 0.05$; **, $P < 0.01$

Table S2. Serum chemical parameters of SD rats in the control and SCCPs-treated groups (*n*= 10, mean ± standard error).

Characters	Dose (mg/kg bm/d)			
	0	0.01	1	100
ALP (U/L)	295 ± 67	247 ± 37	249 ± 72	264 ± 75
ALT (U/L)	46 ± 22	42 ± 7	46 ± 15	52 ± 27
AST (U/L)	74 ± 30	70 ± 8	73 ± 14	74 ± 17
UREA (mmol/L)	7.3 ± 1.3	6.9 ± 1.1	7.6 ± 1.2	6.9 ± 1.0
CREA (μmol/L)	30 ± 3	28 ± 3	29 ± 3	27 ± 2
T-BIL (μmol/L)	0.3 ± 0.3	0.3 ± 0.2	0.4 ± 0.3	0.3 ± 0.3
GLU (mmol/L)	10.5 ± 1.9	8.6 ± 1.4	8.5 ± 2.0*	9.3 ± 1.1
CHO (mmol/L)	1.1 ± 0.3	1.1 ± 0.2	1.1 ± 0.2	1.0 ± 0.2
TP (g/L)	61.8 ± 2.0	62.3 ± 2.5	64.4 ± 2.7	63.0 ± 4.0
ALB (g/L)	39.4 ± 1.5	38.7 ± 1.6	40.4 ± 1.3	39.8 ± 2.0
LDH (U/L)	190 ± 106	153 ± 21	98 ± 20**	169 ± 52
TG (mmol/L)	0.4 ± 0.08	0.4 ± 0.09	0.3± 0.09	0.4 ± 0.1
Ca^{2+} (mmol/L)	2.9 ± 0.08	2.8 ± 0.09	2.8 ± 0.06	3.0 ± 0.2
K^{+} (mmol/L)	6.7 ± 0.7	7.2 ± 0.4	6.7 ± 0.5	7.3± 0.4
Na^{+} (mmol/L)	141 ± 2	141 ± 2	142 ± 1	140 ± 2
Cl^{-} (mmol/L)	89 ± 1	89 ± 1	90 ± 1	89 ± 1
CK (U/L)	196 ± 48	181 ± 26	136 ± 20**	162 ± 25
GLB (g/L)	22.4 ± 1.4	23.6 ± 1.9	24.0 ± 1.7	23.2 ± 2.2
A/G	1.8 ± 0.1	1.7 ± 0.2	1.7 ± 0.1	1.8 ± 0.2
UA (μmol/L)	1.3 ± 0.6	1.2 ± 0.5	1.2 ± 0.3	1.7 ± 0.5

Note: ALP (alkaline phosphatase), ALT (Alanine Transaminase), AST (aspartate aminotransferase), UREA (urea nitrogen), CREA (creatinine), T-BIL (total bilirubin), GLU (Glucose), CHO (cholesterol), TP (total protein), ALB (albumin), LDH (lactate dehydrogenase), TG (triglyceride), Ca^{2+} (calcium), K^{+} (potassium), Na^{+} (sodium), Cl^{-} (chlorine), CK (creatine kinase), GLB (globulin), A/G (albumin/globulin), UA (uric acid).*, $P < 0.05$; **, $P < 0.01$.

189 **Table S3.** Routine urinalysis results of SD rats in the control and SCCPs-treated groups (*n*= 10,
190 mean ± standard error).

Characters	Dose (mg/kg bm/d)			
	0	0.01	1	100
KET (mmol/L)	1.50 ± 1.03	1.70 ± 1.30	1.30 ± 1.11	2.00 ± 1.47
PRO (g/L)	1.25 ± 0.98	1.58 ± 1.26	1.12 ± 1.08	2.52 ± 1.04**
SG	1.02 ± 0.01	1.02 ± 0.00	1.02 ± 0.01	1.02 ± 0.00
pH	6.45 ± 0.64	6.50 ± 0.53	6.35 ± 0.78	6.80 ± 0.95
Vc (mmol/L)	1.64 ± 1.68	1.24 ± 1.65	1.24 ± 1.90	1.72 ± 2.11

191 Note: KET (Ketone), PRO (Protein), SG (Specific Gravity), Vc (Vitamin C). **, $P < 0.01$

192 **Table S4.** Result of quantitative RT-PCR validation.

Gene symbol	Genebank Accession	Dose (mg/kg bm/d)	Microarray *P* value	Microarray FC	RT-PCR *P* value	RT-PCR FC
Cdk1	NM_019296	0.01	0.0147	0.4104	0.0106	0.4276
Ednra	NM_012550	0.01	0.0023	0.1924	0.0130	0.2022
Pfkfb1	NM_012621	1	0.0331	2.5485	0.0680	2.3939
Slpi	NM_053372	1	0.0338	2.1898	0.0182	2.1510
Herpud1	NM_053523	1	0.0193	2.1191	0.0040	2.1272
Acaa1b	NM_001040019	100	0.0011	4.5918	0.0009	4.4520
Alas1	NM_024484	100	0.0025	2.3848	0.0164	1.7311
Acot2	NM_138907	100	0.0030	3.2447	0.0039	2.8847

193

194 **Table S5.** Sixty three differentially expressed genes encoding hepatic enzymes in livers of rats
195 exposed to SCCPs.

	Gene	Coded enzyme	Related pathway
1	Akr1b8	aldo-keto reductase family 1, member B8	Fructose and mannose metabolism Galactose metabolism Glycerolipid metabolism Folate biosynthesis
2	Aacs	acetoacetyl-CoA synthetase	Butanoate metabolism Valine, leucine and isoleucine degradation
3	Acaa1a	acetyl-CoA acyltransferase 1A	Fatty acid degradation Valine, leucine and isoleucine degradation alpha-Linolenic acid metabolism Biosynthesis of unsaturated fatty acids Fatty acid metabolism
4	Acaa1b	acetyl-CoA acyltransferase 1B	Fatty acid degradation Valine, leucine and isoleucine degradation alpha-Linolenic acid metabolism Biosynthesis of unsaturated fatty acids Fatty acid metabolism
5	Acer2	alkaline ceramidase 2	Sphingolipid metabolism
6	Acnat1	acyl-coenzyme A amino acid N-acyltransferase 1	Fatty acid conjugation (Reilly et al. 2007)
7	Acot2	acyl-CoA thioesterase 2	Fatty acid elongation Biosynthesis of unsaturated fatty acids
8	Acot8	acyl-CoA thioesterase 8	Primary bile acid biosynthesis
9	Acsm5	acyl-CoA synthetase medium-chain family member 5	Butanoate metabolism
10	Adcy10	adenylate cyclase 10	Purine metabolism
11	Adh4	alcohol dehydrogenase 4	Glycolysis / Gluconeogenesis Fatty acid degradation Tyrosine metabolism Retinol metabolism Metabolism of xenobiotics by cytochrome P450 Drug metabolism - cytochrome P450
12	Adh7	alcohol dehydrogenase 7	Glycolysis / Gluconeogenesis Fatty acid degradation Tyrosine metabolism Retinol metabolism Metabolism of xenobiotics by cytochrome P450 Drug metabolism - cytochrome P450
13	Akr1d1	aldo-keto reductase family 1, member D1	Primary bile acid biosynthesis Steroid hormone biosynthesis

14	Alas1	5-aminolevulinate synthase 1	Glycine, serine and threonine metabolism Porphyrin and chlorophyll metabolism
15	Aldh1a1	aldehyde dehydrogenase 1 family, member A1	Retinol metabolism
16	Amacr	alpha-methylacyl-CoA racemase	Primary bile acid biosynthesis
17	Aox3	aldehyde oxidase 3	Valine, leucine and isoleucine degradation Tyrosine metabolism Tryptophan metabolism Vitamin B6 metabolism Nicotinate and nicotinamide metabolism Retinol metabolism
18	Asah2	N-acylsphingosine amidohydrolase 2	Sphingolipid metabolism
19	Atp5hl1	ATP synthase, H+ transporting, mitochondrial Fo complex, subunit d-like 1	
20	Bcmo1	beta-carotene oxygenase 1	Retinol metabolism
21	Car3	carbonic anhydrase 3	Nitrogen metabolism
22	Cpt1b	carnitine palmitoyltransferase 1B	Fatty acid degradation Fatty acid metabolism
23	Crat	carnitine O-acetyltransferase	Peroxisome
24	Cyp17a1	cytochrome P450, family 17, subfamily a, polypeptide 1	Steroid hormone biosynthesis
25	Cyp2b12	cytochrome P450, family 2, subfamily b, polypeptide 12	Steroid hormone biosynthesis Arachidonic acid metabolism Retinol metabolism
26	Cyp2j4	cytochrome P450, family 2, subfamily j, polypeptide 4	Arachidonic acid metabolism Linoleic acid metabolism
27	Cyp4a1	cytochrome P450, family 4, subfamily a, polypeptide 1	Fatty acid degradation Arachidonic acid metabolism Retinol metabolism
28	Decr2	2,4-dienoyl-CoA reductase 2	Peroxisome
29	Dhdds	dehydrodolichyl diphosphate synthase subunit	Terpenoid backbone biosynthesis
30	Ech1	enoyl-CoA hydratase 1	Peroxisome
31	Eci1	enoyl-CoA delta isomerase 1	Fatty acid degradation
32	Ehhadh	enoyl-CoA hydratase and 3-hydroxyacyl CoA dehydrogenase	Fatty acid degradation Valine, leucine and isoleucine degradation Lysine degradation Tryptophan metabolism beta-Alanine metabolism Propanoate metabolism Butanoate metabolism Carbon metabolism Fatty acid metabolism Peroxisome

33	Elovl2	ELOVL fatty acid elongase 2	Fatty acid elongation Biosynthesis of unsaturated fatty acids Fatty acid metabolism
34	Elovl6	ELOVL fatty acid elongase 6	Fatty acid elongation Biosynthesis of unsaturated fatty acids Fatty acid metabolism
35	Enpp1	ectonucleotide pyrophosphatase/phosphodiesterase 1	Purine metabolism Pyrimidine metabolism Starch and sucrose metabolism Riboflavin metabolism Nicotinate and nicotinamide metabolism Pantothenate and CoA biosynthesis
36	Enpp3	ectonucleotide pyrophosphatase/phosphodiesterase 3	Purine metabolism Pyrimidine metabolism Starch and sucrose metabolism Riboflavin metabolism Nicotinate and nicotinamide metabolism Pantothenate and CoA biosynthesis
37	Fads2	fatty acid desaturase 2	alpha-Linolenic acid metabolism Biosynthesis of unsaturated fatty acids Fatty acid metabolism PPAR signaling pathway
38	Fasn	fatty acid synthase	Fatty acid biosynthesis
39	Fbp2	fructose-bisphosphatase 2	Glycolysis / Gluconeogenesis Pentose phosphate pathway Fructose and mannose metabolism
40	Glt1d1	glycosyltransferase 1 domain containing 1	
41	Gnpda2	glucosamine-6-phosphate deaminase 2	Amino sugar and nucleotide sugar metabolism
42	Gpd2	glycerol-3-phosphate dehydrogenase 2	Glycerophospholipid metabolism
43	Gpx3	glutathione peroxidase 3	Glutathione metabolism Arachidonic acid metabolism Thyroid hormone synthesis
44	Gstm5	glutathione S-transferase, mu 5	Glutathione metabolism
45	Hadhb	hydroxyacyl-CoA dehydrogenase/ 3-ketoacyl-CoA thiolase/enoyl-CoA hydratase	Fatty acid elongation Fatty acid degradation Valine, leucine and isoleucine degradation
46	Hao2	hydroxyacid oxidase 2	Glyoxylate and dicarboxylate metabolism
47	Hibch	3-hydroxyisobutyryl-CoA hydrolase	Valine, leucine and isoleucine degradation beta-Alanine metabolism Propanoate metabolism
48	Hmgcr	3-hydroxy-3-methylglutaryl-CoA reductase	Terpenoid backbone biosynthesis Bile secretion
49	Lpin1	phosphatidate phosphatase LPIN 1	Glycerolipid metabolism

			Glycerophospholipid metabolism
50	Lpin2	phosphatidate phosphatase LPIN 2	Glycerolipid metabolism Glycerophospholipid metabolism
51	Me1	malic enzyme 1	Pyruvate metabolism
52	Nampt	nicotinamide phosphoribosyltransferase	Nicotinate and nicotinamide metabolism
53	Neu2	neuraminidase2	Sphingolipid metabolism
54	Pklr	pyruvate kinase, liver and RBC	Glycolysis / Gluconeogenesis Purine metabolism Pyruvate metabolism Metabolic pathways Carbon metabolism Biosynthesis of amino acids
55	Pla2g16	phospholipase A2, group XVI	Glycerophospholipid metabolism Ether lipid metabolism Arachidonic acid metabolism Linoleic acid metabolism alpha-Linolenic acid metabolism
56	Pold2	DNA polymerase delta 2, accessory subunit	Purine metabolism Pyrimidine metabolism
57	Ppcdc	phosphopantothenoylcysteine decarboxylase	Pantothenate and CoA biosynthesis
58	Prim1	primase (DNA) subunit 1	Purine metabolism Pyrimidine metabolism
59	Sdr42e1	short chain dehydrogenase/reductase family 42E, member 1	
60	Srd5a2	steroid 5 alpha-reductase 2	Steroid hormone biosynthesis
61	Sult2a1	sulfotransferase family 2A member 1	Metabolism of xenobiotics by cytochrome P450 Bile secretion
62	Tdo2	tryptophan 2,3-dioxygenase	Tryptophan metabolism
63	Vnn1	vanin 1	Pantothenate and CoA biosynthesis

Table S6. The differentially expressed metabolites with VIP > 1 and $P < 0.05$ in livers of rats exposed to SCCPs base on ANOVA.

Metabolites	VIP	P	FDR	log2 (FC)		
				Dose (mg/kg bm/d)		
				0.01	1	100
LysoPC (18:0)	1.68	3.50E-14	1.51E-12	-0.15	-0.4	-0.51
PC (32:4)	1.67	3.21E-19	2.21E-16	0.38	1.33	2.29
LysoPC (18:3(6Z,9Z,12Z))	1.67	6.50E-14	2.48E-12	-0.2	-0.53	-0.67
ADP	1.66	4.24E-18	1.46E-15	-0.09	1.12	1.51
Docosahexaenoic acid	1.65	3.87E-13	1.27E-11	-0.13	-0.66	-1.3
Eicosenoic acid	1.61	4.43E-11	5.86E-10	-0.32	-0.58	-1.12
Dipalmitoylphosphatidic acid	1.6	2.60E-12	5.97E-11	0.16	0.85	1.33
(EZ)-Eicosenoic acid	1.59	2.53E-10	2.60E-09	-0.29	-0.59	-1.15
Melissic acid A	1.57	4.87E-13	1.46E-11	0.06	0.51	1.05
Guanine	1.55	1.76E-10	1.89E-09	-0.1	-0.89	-1.95
2-Methylhippuric acid	1.55	2.75E-10	2.78E-09	-0.27	-1.79	-3.14
PC (36:6)	1.55	5.67E-10	5.06E-09	0.32	0.94	1.14
MG (18:0/0:0/0:0)	1.54	2.39E-09	1.64E-08	-0.33	-0.87	-2.03
MG (16:0/0:0/0:0)	1.53	5.79E-09	3.65E-08	-0.34	-0.7	-1.43
SM (d18:1/18:1(9Z))	1.53	2.80E-11	3.93E-10	0.7	0.72	1.39
PC (14:0/14:0)	1.53	6.24E-15	4.29E-13	0.53	1.07	2.52
Tetracosatetraenoic acid (24:4n-6)	1.52	7.85E-09	4.74E-08	-0.29	-1	-2.03
PC (34:2)	1.51	6.39E-09	3.96E-08	-0.27	-0.42	-0.61
Oxidized glutathione	1.5	2.47E-14	1.31E-12	0.69	1.89	1.7
Palmitic acid	1.5	7.90E-10	6.55E-09	-0.21	-1.59	-1.96
AEA	1.49	1.13E-11	1.70E-10	0	-2.13	-2.72
LysoPC (20:4(5Z,8Z,11Z,14Z))	1.47	1.48E-08	8.54E-08	-0.33	-1.52	-2.02
PE (20:2(11Z,14Z)/18:0)	1.47	4.74E-09	3.08E-08	0.44	0.57	1.15
SM (d18:1/22:1(13Z))	1.47	2.38E-11	3.41E-10	0.38	0.4	1.13
Coenzyme Q10	1.46	4.02E-08	2.03E-07	0.54	0.71	1.12
PEA	1.46	2.09E-10	2.18E-09	0.01	-2.07	-2.86
LysoPC (20:5(5Z,8Z,11Z,14Z,17Z))	1.46	7.87E-10	6.55E-09	-0.32	-0.71	-0.67

Phenylalanine	1.45	3.38E-08	1.76E-07	-0.1	-0.97	-1.7
PC (34:3)	1.44	9.94E-08	4.35E-07	-0.14	-0.43	-0.94
p-Cresol sulfate	1.42	3.27E-07	1.26E-06	-0.3	-0.84	-2.18
L-threonine	1.4	1.35E-09	1.03E-08	-0.63	-0.88	-0.93
Asparagine	1.39	3.84E-09	2.58E-08	-0.8	-1.19	-1.27
SM (d18:0/16:1(9Z)(OH))	1.39	2.01E-07	8.15E-07	0.66	0.7	1.04
CoA	1.38	1.01E-07	4.38E-07	0.08	0.39	0.85
(Z)-9-Heptadecenoic acid	1.37	3.09E-07	1.20E-06	-0.04	-0.5	-1.39
6Z,9Z,12Z-Octadecatrienoic acid	1.36	6.49E-08	3.00E-07	-0.13	-0.23	-0.97
Valerylcarnitine	1.35	1.53E-08	8.72E-08	0.3	0.47	1.37
PC (38:5)	1.35	1.69E-06	5.14E-06	-0.08	-0.24	-0.56
Pregnenolone	1.35	4.44E-12	9.25E-11	-0.01	-1.07	-0.72
Nonadeca-10(Z)-enoic acid	1.35	2.84E-08	1.49E-07	0.1	-0.39	-1.44
Tetradecanoylcarnitine	1.34	6.48E-06	1.66E-05	-0.24	-0.64	-1.04
L-serine	1.34	2.34E-09	1.64E-08	-0.56	-0.81	-0.75
PC (32:2)	1.31	4.67E-06	1.26E-05	-0.13	-0.46	-0.53
Aldosterone	1.31	6.98E-07	2.39E-06	-0.64	-0.68	-1.1
PC (30:1)	1.31	5.59E-06	1.47E-05	-0.07	-0.25	-0.56
Pentadecanoic acid	1.31	1.46E-06	4.57E-06	-0.07	-0.32	-1.07
Alanine	1.31	1.88E-07	7.64E-07	-0.48	-0.69	-0.72
Thymine	1.3	3.78E-07	1.44E-06	-1	-1.69	-1.82
SM (d18:0/18:1(9Z))	1.29	8.97E-09	5.37E-08	0.27	0.16	0.71
Sarcosine	1.29	5.21E-07	1.88E-06	-0.48	-0.68	-0.73
Valine	1.27	3.28E-07	1.26E-06	-0.5	-0.66	-0.7
Proline	1.27	3.66E-07	1.40E-06	-0.5	-0.67	-0.7
Tyrosine	1.26	6.44E-07	2.24E-06	-0.58	-0.73	-0.82
CerP (d18:1/24:1(15Z))	1.48	7.13E-09	4.34E-08	0.21	1	1.4
L-ornithine	1.25	4.82E-08	2.35E-07	-0.72	-0.78	-0.87
Tetracosapentaenoic acid (24:5n-3)	1.25	3.30E-05	7.00E-05	-0.15	-1.1	-2.46
LysoPC (22:6 (4Z,7Z,10Z,13Z,16Z,19Z))	1.25	4.03E-08	2.03E-07	-0.25	-0.12	-0.6
Cis-5-Tetradecenoylcarnitine	1.25	1.70E-08	9.51E-08	0.57	0.6	2.62
PC (15:0/18:1(11Z))	1.24	2.37E-09	1.64E-08	0.24	0.7	0.5

Aspartate	1.24	2.52E-05	5.60E-05	-0.3	-0.54	-0.61
PC (31:0)	1.24	2.70E-05	5.95E-05	0.71	0.76	1.26
L-Methionine	1.24	3.83E-08	1.97E-07	-0.71	-0.73	-0.83
PC (38:4)	1.24	7.32E-05	1.43E-04	-0.16	-0.27	-0.53
PC (18:2(9Z,12Z)/15:0)	1.22	2.61E-07	1.05E-06	0.49	0.76	0.64
10E,12Z-Octadecadienoic acid	1.21	1.53E-04	2.73E-04	-0.2	-0.44	-0.73
Xanthosine	1.21	7.29E-07	2.47E-06	0.16	-0.25	-0.99
Stearamide	1.21	1.70E-04	3.00E-04	-0.25	-0.45	-0.83
11,14,17-Eicosatrienoic acid	1.21	1.38E-04	2.50E-04	-0.29	-1.09	-1.66
Arachidonic acid	1.2	1.13E-06	3.60E-06	0.07	-0.15	-0.79
Deoxycytidine	1.2	3.66E-06	1.01E-05	-0.46	-0.71	-0.67
LysoPE (18:2(9Z,12Z)/0:0)	1.2	3.90E-07	1.47E-06	0.05	0.11	0.74
Oleic acid	1.2	1.07E-05	2.59E-05	0.1	-0.5	-0.87
Pentacosanoic acid	1.2	8.18E-05	1.58E-04	-0.04	-0.56	-1.09
Methylmalonylcarnitine	1.19	1.21E-09	9.49E-09	-0.11	-0.04	0.95
Linoelaidyl carnitine	1.17	1.56E-04	2.77E-04	0.1	0.61	0.93
PE (36:4)	1.17	1.24E-05	2.97E-05	0.29	0.21	0.6
SM (d18:1/20:0)	1.26	5.10E-06	1.37E-05	0.38	0.35	0.66
SM (d18:1/16:0)	1.16	2.53E-04	4.34E-04	-0.04	-0.19	-0.31
PC (32:1)	1.16	1.69E-04	3.00E-04	0.11	0.32	0.34
21-Deoxycortisol	1.15	2.74E-06	7.88E-06	0.21	-1.26	-1.35
SM (d18:1/14:0)	1.15	1.24E-04	2.28E-04	0.27	0.56	0.55
PE (34:1)	1.14	3.89E-04	6.32E-04	0.19	0.27	0.52
LysoPC (18:1(11Z))	1.14	4.91E-07	1.80E-06	0.41	0.82	0.6
3-Aminoisobutanoic acid	1.13	3.02E-04	5.06E-04	-0.45	-1.16	-1.18
Uric acid	1.13	5.32E-04	8.31E-04	-0.2	-1.09	-2.55
L-Malic acid	1.13	2.06E-06	6.16E-06	0.19	-0.17	-0.79
L-citrulline	1.12	2.90E-06	8.30E-06	-0.51	-0.71	-0.59
LysoPE (18:1(9Z)/0:0)	1.12	1.65E-07	7.05E-07	0.16	0	0.78
Gamma-Aminobutyric acid	1.11	6.08E-04	9.42E-04	-0.4	-1.26	-1.45
Tetracosahexaenoic acid	1.11	2.70E-04	4.61E-04	0.05	-0.71	-2.01
LysoPC (18:2(9Z,12Z))	1.11	1.38E-05	3.25E-05	0.96	1.43	1.22

Cytosine	1.1	2.09E-06	6.20E-06	-0.59	-0.68	-0.63
Fructose 6-phosphate	1.1	3.50E-05	7.35E-05	-0.71	-0.82	-0.91
Deoxyinosine	1.1	1.30E-03	1.87E-03	-0.38	-0.92	-1.41
Eicosapentaenoic acid	1.09	5.51E-04	8.60E-04	-0.1	-0.26	-0.77
SM (d18:1/24:1(15Z))	1.09	1.12E-06	3.60E-06	0.21	0.04	0.65
Leu-Pro	1.09	2.51E-04	4.30E-04	-0.41	-0.33	-0.96
Succinic acid	1.09	2.57E-06	7.46E-06	0.27	-0.32	-0.7
Lactic acid	1.09	1.01E-03	1.48E-03	-0.4	-0.99	-1.18
PC (38:7)	1.08	2.98E-04	5.01E-04	0.07	0.66	0.67
Xanthine	1.08	5.01E-05	1.03E-04	0.21	-0.41	-1.07
LysoPE (22:4(7Z,10Z,13Z,16Z)/0:0)	1.08	3.72E-05	7.77E-05	1.58	1.41	1.77
LysoPC (20:3(5Z,8Z,11Z))	1.07	2.43E-04	4.19E-04	0.02	0.39	0.38
3, 5-Tetradecadiencarnitine	1.07	1.92E-04	3.37E-04	-0.68	-0.46	-2.27
Oxoglutaric acid	1.07	2.65E-06	7.67E-06	0.31	-0.24	-0.88
L-glutamine	1.07	8.44E-04	1.27E-03	-0.26	-0.34	-0.44
PC (40:5)	1.07	1.35E-05	3.20E-05	0.18	0.88	0.66
Deoxyguanosine	1.07	4.34E-05	8.94E-05	-0.59	-0.38	-0.84
(R)-3-Hydroxy-hexadecanoic acid	1.07	1.34E-03	1.90E-03	-0.4	-0.59	-0.83
LysoPE (16:1(9Z)/0:0)	1.06	5.04E-05	1.03E-04	0.33	0.19	0.94
PE (18:1(11Z)/18:1(9Z))	1.04	7.04E-07	2.40E-06	-0.18	-0.03	0.56
Stearic acid	1.04	3.31E-05	7.00E-05	-0.41	-1.01	-0.64
1-O-(1Z-hexadecenyl)-2-(4Z,7Z,10Z,13Z,16Z,19Z-docosahexaenoyl)-sn-glycero-3-phosphoethanolamine	1.03	6.45E-04	9.97E-04	0.05	0.15	0.5
Phenol sulphate	1.02	7.99E-05	1.55E-04	0.31	-0.29	-1.71
Lysine	1.02	1.21E-03	1.76E-03	-0.25	-0.35	-0.39
Cysteine	1.01	9.71E-04	1.43E-03	-0.37	-0.31	-0.62
DG(22:6(4Z,7Z,10Z,13Z,16Z,19Z)/22:6(4Z,7Z,10Z,13Z,16Z,19Z)/0:0)	1	4.25E-07	1.58E-06	0.02	0.17	-2.98
Glucose	0.98	1.11E-04	2.08E-04	-0.02	-0.03	-0.96

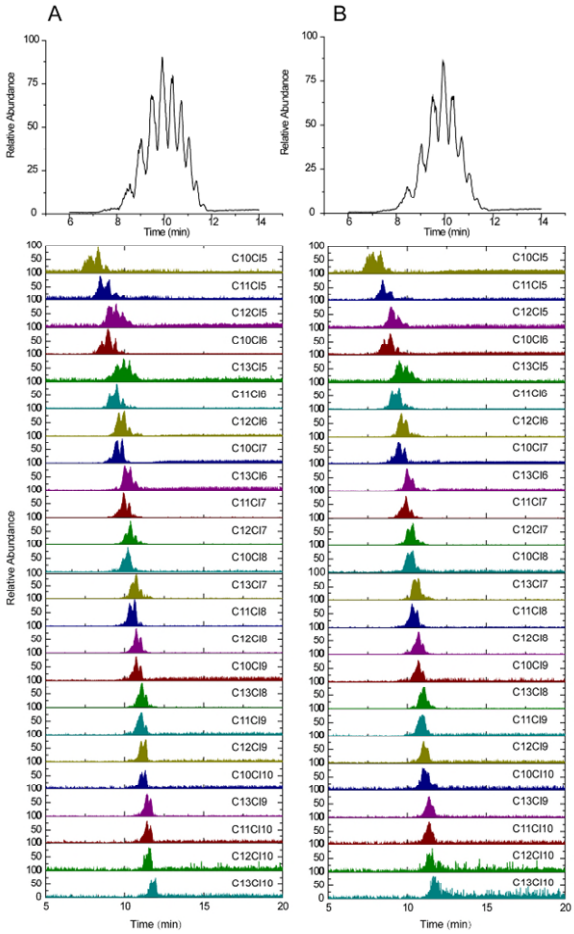

Figure. S1. GC-ECNI-MS chromatograms and extracted ion chromatogram for SCCPs congeners. (A) $C_{10\text{-}13}$-CP with 56.5%Cl synthesized in our laboratory and used in animal studies. (B) $C_{10\text{-}13}$-CP with 55.5%Clobtained from Dr. Ehrenstorfer.

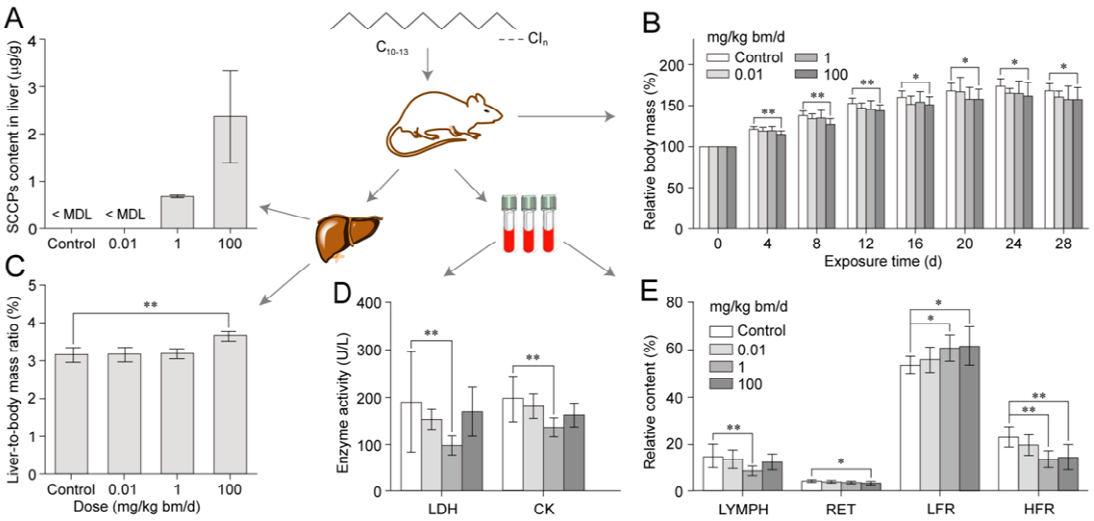

204

205 **Figure S2.** General pathophysiological results for male SD rat exposed to SCCPs for 28 days. (*A*)
206 Concentrations of SCCPs in SD rat liver after 28-day oral administration (n = 3, mean ± standard error).
207 (*B*) Changes in body mass of SD rats during 28-day oral administration of SCCPs (n = 10, mean ±
208 standard error). (*C*) Liver-to-body mass ratio of SD rats after 28-day oral administration of SCCPs (n =
209 10, mean ± standard error). (*D*) and (*E*) Hematological parameters of SD rats with significant changes
210 after exposure to SCCPs (n = 10, mean ± standard error). LDH (lactate dehydrogenase), CK (creatine
211 kinase), LYMPH（lymphocyte count），RET (reticulocyte count), LFR (low fluorescent reticulocyte),
212 HFR (high fluorescent reticulocyte). * $P < 0.05$; ** $P < 0.01$.

213

214

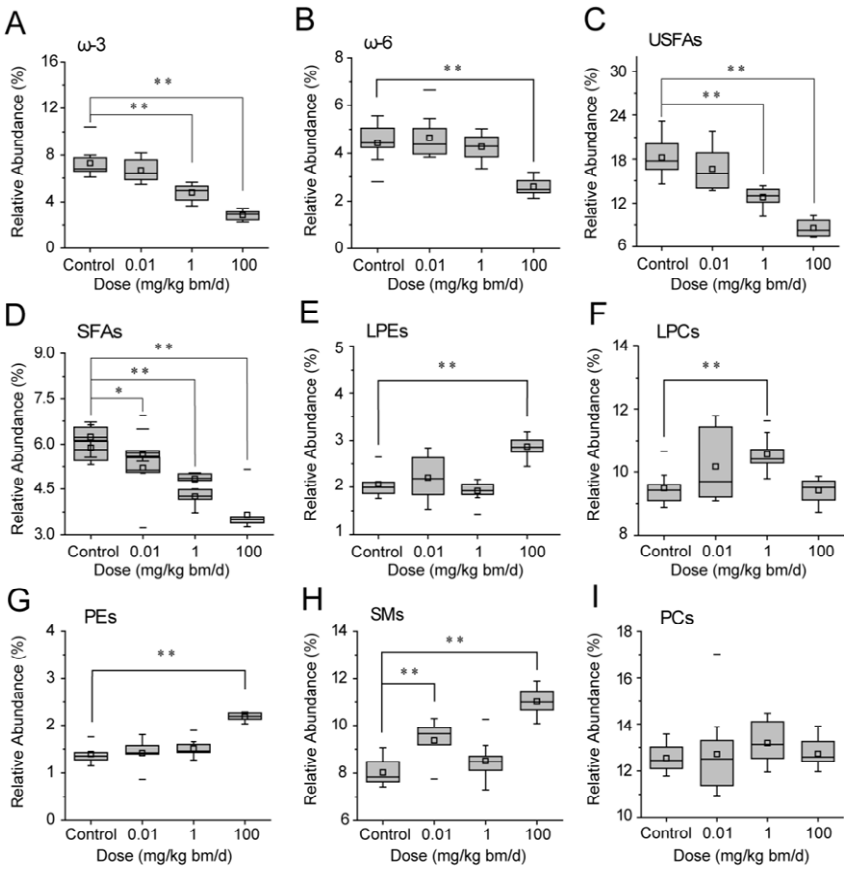

Figure. S3. The most relevant metabolites perturbed by SCCPs in lipid metabolism.(A) and (B) Polyunsaturated ω-6, ω-3 fatty acids in livers of rat f exposed to the various doses of SCCPs, the ω-6 fatty acids shows down-regulation on high dose group, and ω-3 fatty acids shows down-regulation both on low and high dose. (C) and (D) Down-regulation of USFAs and SFAs with increased SCCPs doses. (E) to (I) Lipids metabolism disorder were character by the up-regulation of SMs in livers of rats exposed to very-low and high dose SCCPs, and up-regulation of PEs and LysoPEs in livers of rats exposed to high dose SCCPs, down-regulation of LysoPCs in livers of rats exposed to low dose SCCPs and no significant variation for PC. USFA: unsaturated fatty acid; SFA: saturated fatty acid; SM: sphingomyelin; PC: phosphatidyl choline; LysoPC: lysophosphatidyl choline; PE: phosphatidyl ethanolamine; LysoPE: lysophosphatidyl ethanolamine. *, $P < 0.05$; **, $P < 0.01$.

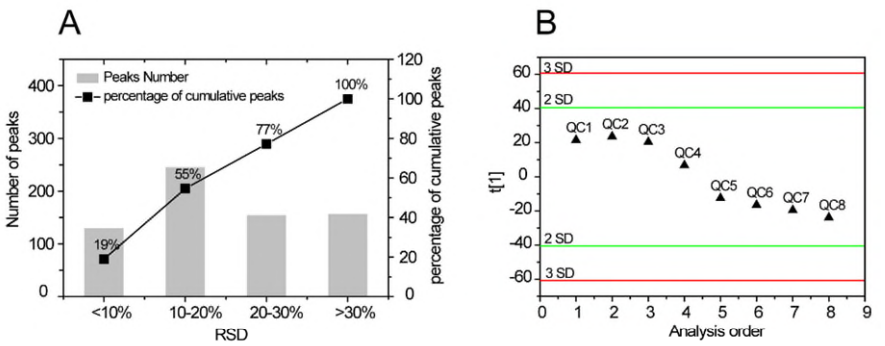

227

228 **Figure. S4**. Distribution of % RSD (A) and score plots of PCA (B) for QC samples. RSD: the
229 relative standard deviation; QC: quality control; PCA: principal component analysis.

Supplemental References

Gou, N., Gu, A.Z., 2011. A New Transcriptional effect level index (TELI) for toxicogenomics-based toxicity assessment. Environ. Sci. Technol. 45, 5410-5417. https://doi.org/10.1021/es200455p.

Peters, J.M., Cattley, R.C., Gonzalez, F.J., 1997. Role of PPAR alpha in the mechanism of action of the nongenotoxic carcinogen and peroxisome proliferator Wy-14,643. Carcinogenesis 18, 2029-2033. https://doi.org/10.1093/carcin/18.11.2029.

Reilly, S-J., O'Shea, E.M., Andersson, U., O'Byrne, J., Alexson, S.E.H., Hunt, M.C., 2007. A peroxisomal acyltransferase in mouse identifies a novel pathway for taurine conjugation of fatty acids. Faseb J. 21, 99-107. https://doi.org/10.1096/fj.06-6919com.

Riedl J, Schreiber R, Otto M, Heilmeier H, Altenburger R, Schmitt-Jansen M. 2015. Metabolic effect level index links multivariate metabolic fingerprints to ecotoxicological effect assessment. Environ. Sci. Technol. 49, 8096-8104. https://doi.org/10.1021/acs.est.5b01386.